HAL
open science

A thermodynamic model of mixed organic-inorganic aerosols to predict activity coefficients

A. Zuend, C. Marcolli, B. P. Luo, Th. Peter

To cite this version:

A. Zuend, C. Marcolli, B. P. Luo, Th. Peter. A thermodynamic model of mixed organic-inorganic aerosols to predict activity coefficients. Atmospheric Chemistry and Physics Discussions, 2008, 8 (2), pp.6069-6151. hal-00304058

HAL Id: hal-00304058

https://hal.science/hal-00304058v1

Submitted on 18 Jun 2008

HAL is a multi-disciplinary open access archive for the deposit and dissemination of scientific research documents, whether they are published or not. The documents may come from teaching and research institutions in France or abroad, or from public or private research centers.

L'archive ouverte pluridisciplinaire **HAL**, est destinée au dépôt et à la diffusion de documents scientifiques de niveau recherche, publiés ou non, émanant des établissements d'enseignement et de recherche français ou étrangers, des laboratoires publics ou privés.

Atmos. Chem. Phys. Discuss., 8, 6069–6151, 2008
www.atmos-chem-phys-discuss.net/8/6069/2008/
© Author(s) 2008. This work is distributed under
the Creative Commons Attribution 3.0 License.

Atmospheric Chemistry and Physics Discussions

A thermodynamic model of mixed organic-inorganic aerosols to predict activity coefficients

A. Zuend, C. Marcolli, B. P. Luo, and Th. Peter

Institute for Atmospheric and Climate Science, ETH Zurich, Switzerland

Received: 20 February 2008 – Accepted: 20 February 2008 – Published: 26 March 2008

Correspondence to: A. Zuend (andreas.zuend@env.ethz.ch)

Published by Copernicus Publications on behalf of the European Geosciences Union.

Abstract

Tropospheric aerosols contain mixtures of inorganic salts, acids, water, and a large variety of organic compounds. Interactions between these substances in liquid mixtures lead to discrepancies from ideal thermodynamic behaviour. By means of activity coefficients, non-ideal behaviour can be taken into account. We present here a thermodynamic model named AIOMFAC (Aerosol Inorganic–Organic Mixtures Functional groups Activity Coefficients) that is able to calculate activity coefficients covering inorganic, organic, and organic–inorganic interactions in aqueous solutions over a wide concentration range. This model is based on the activity coefficient model LIFAC by Yan et al. (1999) that we modified and reparametrised to better describe atmospherically relevant conditions and mixture compositions. Focusing on atmospheric applications we considered H^+, Li^+, Na^+, K^+, NH_4^+, Mg^{2+}, Ca^{2+}, Cl^-, Br^-, NO_3^-, HSO_4^-, and SO_4^{2-} as cations and anions and a wide range of alcohols/polyols composed of the functional groups CH_n and OH as organic compounds. With AIOMFAC, the activities of the components within an aqueous electrolyte solution are well represented up to high ionic strength. Most notably, a semi-empirical middle-range parametrisation of direct organic–inorganic interactions in alcohol + water + salt solutions strongly improves the agreement between experimental and modelled activity coefficients. At room temperature, this novel thermodynamic model offers the possibility to compute equilibrium relative humidities, gas/particle partitioning and liquid–liquid phase separations with high accuracy. In further studies, other organic functional groups will be introduced. The model framework is not restricted to specific ions or organic compounds and is therefore also applicable for other research topics.

1 Introduction

Tropospheric aerosols are composed of many different organic and inorganic substances originating from direct emission of particles and from condensation of gas

ACPD

8, 6069–6151, 2008

phase species (Kanakidou et al., 2005). Field measurements show that organics are not just traces in individual aerosol particles, but rather that 30% to more than 80% of the aerosol mass in the free troposphere are carbonaceous material. Most of this carbonaceous material is organic (Murphy et al., 2006). The abundance of organics in aerosols is comparable to the other well-known tropospheric aerosol components such as sulphuric acid and ammonia. Single particle measurements suggest that organic and inorganic species are mostly internally mixed, especially far away from local sources (Murphy and Thomson, 1997; Middlebrook et al., 1998; Lee et al., 2002; Murphy et al., 2006). This assumption of aerosols as internal mixtures of organics and inorganics is also supported by gas phase diffusion considerations of semi-volatile species (Marcolli et al., 2004). While the prevalent inorganic aerosol constituents are relatively small in number, the organic fraction is highly complex, containing hundreds of compounds with a large fraction still unidentified (Rogge et al., 1993). Such a wide variety of organic compounds in the liquid and solid aerosol phases requires some classification. This is often done considering different functional groups implying that semi-volatile, oxidised organics tend to contain a high degree of functionality, including hydroxyl, carboxyl, and carbonyl groups (Decesari et al., 2000; Maria et al., 2004).

While the thermodynamics of aqueous inorganic systems at atmospheric temperatures is well established, little is known about the physicochemistry of mixed organic–inorganic particles. Salting-out and salting-in effects result from organic–inorganic interactions and are used to improve industrial separation processes. In the atmosphere, they may influence the aerosol phases. Phase separations into a mainly polar (aqueous) and a less polar organic phase as simulated by Erdakos and Pankow (2004) and Chang and Pankow (2006), may considerably influence the gas/particle partitioning of semi-volatile substances compared to a single phase estimation. Recent experiments show that the interactions between inorganic ions and organic compounds in aerosol particles may induce a liquid–liquid phase separation during humidity cycles (Marcolli and Krieger, 2006). Thus, a thermodynamic model is required that predicts the phase partitioning of organic compounds between the gas and the condensed phases, as

well as the compositions of the possible liquid and solid phases at thermodynamic equilibrium.

Non-ideal thermodynamic behaviour in mixtures is usually described by an expression for the excess Gibbs energy $G^{ex}(p, T, n_j)$, as the characteristic state variables of experiments are usually pressure p and temperature T. The corresponding activity coefficients γ_j of the species with amount of moles n_j in the mixture, are related to G^{ex} by:

$$\ln \gamma_j = \left(\frac{\partial G^{ex}/RT}{\partial n_j} \right)_{T,p,n_{j' \neq j}} . \quad (1)$$

For aqueous electrolyte solutions, Pitzer ion-interaction models are well-known for their ability to calculate activity coefficients in aqueous electrolyte solutions, ranging up to high concentrations (Pitzer, 1991; Carslaw et al., 1995; Clegg et al., 1998a). For organic systems, the UNIFAC model, a group-contribution method for predicting liquid-phase activity coefficients of organic mixtures (and water), is widely used (Fredenslund et al., 1975). The model LIQUAC (Li et al., 1994) and its group-contribution version LIFAC by Yan et al. (1999) merge a Pitzer-like approach with a UNIQUAC/UNIFAC model to calculate the activity coefficients of mixed organic–inorganic systems. To resolve the problem of liquid–liquid equilibria (LLE) calculations when using variable reference states in mixed solutions, a modified version of LIQUAC/LIFAC with fixed reference states was proposed recently (Kiepe et al., 2006). Such models enable the computation of chemical potentials and the Gibbs energy of mixed systems, and therefore possible phase separations. The original LIFAC model was developed for chemical engineering purposes, which differ mainly in the selection of chemical species, the concentration, and temperature ranges from the needs of aerosol science.

In this study, we present a modified LIFAC model to describe atmospherically relevant aqueous solutions up to high ionic concentrations at room temperature. This activity coefficient model named AIOMFAC (Aerosol Inorganic–Organic Mixtures Functional groups Activity Coefficients) explicitly accounts for molecular interaction effects

between solution constituents, both organic and inorganic. In comparison, the ZSR mixing rule (Zdanovskii, 1936, 1948; Stokes and Robinson, 1966) and models based on such rules do not explicitly consider organic–inorganic interactions. The careful choice of reference and standard states (see below) for the neutral and ionic species allows to compute vapour–liquid (VLE), liquid–liquid (LLE) and solid–liquid (SLE) equilibria within one framework.

In the atmosphere, the relative humidity (RH) varies over a wide range and thus affects the concentrations and stable phases in aerosol particles. Unlike in bulk solutions, in liquid aerosol droplets the solution can become highly supersaturated (metastable) with respect to crystalline phases. For this reason, AIOMFAC was parametrised taking such high ionic strengths into account by using also data from electrodynamic balance (EDB) measurements of single levitated particles. Besides choosing more appropriate reference and standard states and accounting for high ionic strength, other differences compared to the original LIFAC model concern the introduction of additional electrolyte species such as sulphuric acid and ammonium bisulphate. Organic compounds used in this study comprise a wide range of alcohols and polyols, represented by the functional groups OH and CH_n (n=0, 1, 2, 3). The presented modular framework allows to include further functional groups, e.g. carboxyl, carbonyl or aromatic groups, in future studies.

2 Model framework

2.1 General considerations

The liquid mixtures considered in the present study are composed of different inorganic salts, inorganic acids, organic compounds, and water at room temperature (298 K). Organics are constrained to alcohols and polyols. As we are primarily interested in describing natural aerosols with their tendency to stay fully liquid despite supersaturations with respect to various associated crystalline states, the formation of solid salts or

hydrates is prevented on purpose, enabling the formation of metastable solutions. The mixtures are treated as homogeneous bulk solutions excluding curvature effects, which become only important for aerosol droplet radii smaller than 50 nm. Using the terminology of Yan et al. (1999), organic components and water are called "solvents" and the term "solute" refers to ions. All salts and acids in the liquid mixture are treated as completely dissociated into ions, except for the second dissociation stage of sulphuric acid ($HSO_4^- \rightleftharpoons H^+ + SO_4^{2-}$) which is explicitly taken into account. Strictly speaking, assuming complete dissociation is valid only at very low solute concentrations because even strong electrolytes associate to a certain amount at higher concentrations (Heyrovska, 2006). However, ion association effects on solution thermodynamics are taken into account by the activity coefficients of the solutes and solvents, thereby justifying the present approach.

2.1.1 Group contribution concept

Following the idea of UNIFAC and LIFAC, a group contribution concept is used to describe interaction effects of organic compounds in a solution, thereby covering a large number of organics by means of just a few functional groups. For the use in the different model parts, the functional groups of a chemical species are further divided into so-called (functional) main groups and subgroups. For example, the alkyl groups CH_3, CH_2, CH and C are different subgroups classified into the main group CH_n. The hydroxyl group OH is the only subgroup of the main group OH. Therefore, 1-propanol ($CH_3-CH_2-CH_2-OH$) consists of $3\times CH_n + 1\times OH$ in terms of main groups – or when resolved into subgroups of $1\times CH_3 + 2\times CH_2 + 1\times OH$.

The group-contribution method is not restricted to organic compounds. In a generalised form it is applied to ions and water too, e.g., in the UNIFAC model part of AIOMFAC the term subgroup is also referring to water and ions. In the cases of water and inorganic ions, main groups, subgroups, and chemical species are in each case identical and the terms are used according to the context. Consequently, the category "solvent main groups" of an aqueous organic–inorganic solution includes the different

main groups of organic solvents as well as water.

2.1.2 Reference states

To avoid problems when using the AIOMFAC model to calculate liquid–liquid phase separations, the reference and standard states of the solvents and solutes should be chosen appropriately. The chemical potential μ_j (J mol^{-1}) of component j in the solution is:

$$\mu_j = \mu_j^\circ + RT \ln a_j, \tag{2}$$

where μ_j° is the chemical potential of j with respect to a standard state, R (J K^{-1} mol^{-1}) the universal gas constant, T (K) the temperature, and a_j the activity of species j. Using indices i for ions and s for solvent components, the mole fraction of j (j used for solvent or solute species) in terms of number of moles n_j is:

$$x_j = \frac{n_j}{\sum_i n_i + \sum_s n_s}. \tag{3}$$

On the mole fraction scale the activity coefficient $\gamma_j^{(x)}$ is related to $a_j^{(x)}$ by:

$$a_j^{(x)} = \gamma_j^{(x)} \frac{x_j}{x_j^\circ}, \tag{4}$$

where the superscript (x) denotes the mole fraction basis and x_j° is the standard state mole fraction of j.

For solvent components we choose the symmetric convention with the standard state of the pure liquid (x_s°=1) and the reference state of $\gamma_s^{(x)} \rightarrow 1$ as $x_s \rightarrow 1$. For ions a pure liquid (of cations or anions) is of course inconceivable. To use the symmetric convention for ions, one would therefore have to choose pure fused salts as the reference states

(Erdakos et al., 2006). However, having more than one species of both cations and anions in a mixture, the reference basis of pure fused salt becomes ambiguous (Pitzer, 1991). To avoid such conditions (and to make use of an experimentally preferred scale), we chose the unsymmetrical convention on the molality basis for the ions.

Molality m_i (mol kg^{-1}) of ion i in a solution with solvent components s is defined as:

$$m_i = \frac{n_i}{\sum_s n_s M_s}, \tag{5}$$

here n_i and n_s are the number of moles of the ionic and solvent components, respectively, and M_s (kg mol^{-1}) is the molar mass of compound s. Similar to Eq. (4), the relation for the activity coefficient on the molality basis (m) is:

$$a_i^{(m)} = \gamma_i^{(m)} \frac{m_i}{m_i^\circ}, \tag{6}$$

with m_i° being the standard state molality (conventionally defined as unit molality, i.e. m_i°=1 kg mol^{-1}). For LLE calculations it is very useful to have the same fixed standard state in all coexisting (liquid) phases of different composition. For atmospheric aerosol systems it makes sense to choose water as the reference solvent. In the AIOMFAC model, the reference state of ions is therefore the infinitely diluted solution of ion i in water: $\gamma_i^{(m)} \rightarrow 1$ as $x_w \rightarrow 1$, $\sum_{s \neq w} x_s \rightarrow 0$, and $m_i \rightarrow 0$, $I \rightarrow 0$, where I is the ionic strength (Eq. 10). In contrast to the symmetric mole fraction convention, where reference state and standard state are equal, in the unsymmetric convention the standard state is the hypothetical ideal aqueous solution of unit molality at standard pressure and temperature.

2.1.3 Non-ideal thermodynamics

The excess Gibbs energy G^{ex} (J) characterises for the non-ideality of a thermodynamic system. Different types of interactions involving charged and non-charged solution

species, interacting over different geometric ranges, can be identified. The total excess Gibbs energy of a multicomponent mixture in the AIOMFAC model is expressed in terms of three contributions from long-range (LR), middle-range (MR) and short-range (SR) interactions:

$$G^{ex} = G^{ex}_{\mathrm{LR}} + G^{ex}_{\mathrm{MR}} + G^{ex}_{\mathrm{SR}}. \tag{7}$$

A detailed description of typical expressions for interaction potentials, which play a role in inorganic mixtures or in organic–inorganic mixtures has been given by, e.g. Pitzer (1991) and Li et al. (1994), respectively. Figure 1 schematically shows the three interaction ranges considered in AIOMFAC. Long-range and middle-range interactions are described within a Pitzer-like part, in which the former are described by an extended Debye-Hückel term. Short-range interactions of non-charged components are calculated in the UNIFAC part. Note that when no electrolytes are in the mixture, AIOMFAC reduces to UNIFAC. In the following sections, the LR, MR, and SR model parts are explained in more detail.

2.2 Long-range contribution

The G^{ex}_{LR} term represents the LR interaction contribution caused by Coulomb electrostatic forces between the permanently charged ions, moderated by the presence of the dielectric solvent medium. The Debye-Hückel theory was the first approach to successfully describe the electrolyte effects in highly diluted solutions (Debye and Hückel, 1923). This theory treats the solutes as electrical charges in a solvent medium of a specific density and dielectric constant and was shown to be correct in the limit of infinite dilution. In this study, we use the extended Debye-Hückel theory modified as by Fowler and Guggenheim (1949). As a consequence of the choice of the reference solvent water for inorganic ions, the Debye-Hückel expression is different from the one in original LIFAC. Instead of using mixing rules to estimate the density and dielectric constant of the solvent mixture, we use water properties for all solvent components. Similar assumptions were made for the LR part of other mixed solvent models (Iliuta

et al., 2000). With this constraint, the corresponding LR activity coefficient expressions for the solvents $\gamma_s^{\mathrm{LR,(x)}}$ and the ions $\gamma_i^{\mathrm{LR,(x),\infty}}$ are:

$$\ln \gamma_s^{\mathrm{LR,(x)}} = \frac{2AM_s}{b^3}\left[1 + b\sqrt{I} - \frac{1}{1+b\sqrt{I}} - 2\ln\left(1 + b\sqrt{I}\right)\right], \tag{8}$$

$$\ln \gamma_i^{\mathrm{LR,(x),\infty}} = \frac{-z_i^2 A\sqrt{I}}{1+b\sqrt{I}}. \tag{9}$$

Equation (9) gives the activity coefficient of ion i in the mole fraction basis (x) with the reference state of infinite dilution in water, indicated by superscript ∞. M_s is the molar mass of solvent s, z_i the number of elementary charges of ion i, and the ionic strength I (mol kg^{-1}) is:

$$I = \frac{1}{2}\sum_i m_i z_i^2. \tag{10}$$

The Debye-Hückel parameters A (kg$^{1/2}$ mol$^{-1/2}$) and b (kg$^{1/2}$ mol$^{-1/2}$), depend on temperature T (K), density ρ_w (kg m^{-3}), and static permittivity ϵ_w (C^2 J^{-1} m^{-1}) of water, as calculated based on a distance of closest approach of 0.4 nm between ions:

$$A = 1.327757 \cdot 10^5 \frac{\sqrt{\rho_w}}{(\epsilon_w T)^{3/2}}, \tag{11}$$

$$b = 6.359696 \frac{\sqrt{\rho_w}}{\sqrt{\epsilon_w T}}, \tag{12}$$

with all variables expressed in SI units as mentioned above. The simplification to a water-properties based expression for LR activity coefficients implicates the advantage of not having to estimate unknown dielectric constants of certain organic compounds (Raatikainen and Laaksonen, 2005) and maintains the thermodynamic consistency

regarding the chosen reference states. In a real mixture solvents have densities and dielectric properties different from those of pure water, which was the reason for other authors to avoid applying this simplification. We compensate inaccuracies stemming from this simplification in the semi-empirical MR part (see below). Also, since the physical validity of the Debye-Hückel equation is limited to highly dilute ionic solutions, the main effect of the LR part and the involved approximations to describe a mixture's behaviour holds only in that concentration range (typically $<0.1\,\mathrm{mol\,kg^{-1}}$).

2.3 Middle-range contribution

The G^{ex}_{MR} term, as illustrated in Fig. 1, is the contribution of the interaction effects involving ions and permanent or induced dipoles. Moreover, the semi-empirical character of the MR part, containing most of the adjustable parameters, can be regarded as the model part, which describes all the interaction effects involving ions not considered by the LR and SR contributions. This includes corrections to assumptions made in the LR and SR parts with respect to approximations of physical parameters. MR interactions of solvent compounds (organics and water) with ions are calculated using functional main groups.

The expression for G^{ex}_{MR} of a mixture containing n_k moles of solvent main groups k (main groups of organics and water), with molar masses M_k, and n_i moles of ions i is:

$$\frac{G^{ex}_{\mathrm{MR}}}{RT} = \frac{1}{\sum_k n_k M_k} \sum_k \sum_i B_{k,i}(I) n_k n_i + \frac{1}{\sum_k n_k M_k} \sum_c \sum_a B_{c,a}(I) n_c n_a + \frac{1}{\sum_k n_k M_k} \sum_c \sum_a C_{c,a}(I) n_c n_a \sum_i \frac{n_i |z_i|}{\sum_k n_k M_k} + \frac{1}{\sum_k n_k M_k} \sum_c \sum_{c' \geq c} R_{c,c'} n_c n_{c'}$$

ACPD
8, 6069–6151, 2008

$$+\frac{1}{\left(\sum_k n_k M_k\right)^2}\sum_c\sum_{c'\geq c}\sum_a Q_{c,c',a}n_c n_{c'} n_a. \tag{13}$$

n_c and $n_{c'}$ are moles of cations, n_a are moles of anions, and I is the ionic strength (Eq. 10). $B_{k,i}(I)$ (kg mol^{-1}) and $B_{c,a}(I)$ (kg mol^{-1}) are binary interaction coefficients between solvent main groups and ions, and between cations and anions, respectively. $C_{c,a}(I)$ (kg^2 mol^{-2}) are interaction coefficients between cation–anion pairs with respect to the total charge concentration. The coefficients $R_{c,c'}$ (kg mol^{-1}) and $Q_{c,c',a}$ (kg^2 mol^{-2}) describe binary and ternary interactions involving two different cations. These latter two interaction coefficients were introduced to improve the description of systems containing sulphuric acid and ammonium sulphate, especially at very high ionic strength. Hence, the last two terms of Eq. (13) vanish in other cases.

Equation (13) could be extended by terms accounting for interactions between two different anions, two different anions and a cation, and so on. We found that it is not necessary to introduce such higher order interaction terms for the solutions studied. The first three interaction coefficients are parametrised as functions of ionic strength I. In contrast to LIFAC, in AIOMFAC we use expressions, which are similar to the ones used for the Pitzer model of Knopf et al. (2003):

$$B_{k,i}(I) = b^{(1)}_{k,i} + b^{(2)}_{k,i}\, e^{-b^{(3)}_{k,i}\sqrt{I}}, \tag{14}$$

$$B_{c,a}(I) = b^{(1)}_{c,a} + b^{(2)}_{c,a}\, e^{-b^{(3)}_{c,a}\sqrt{I}}, \tag{15}$$

$$C_{c,a}(I) = c^{(1)}_{c,a}\, e^{-c^{(2)}_{c,a}\sqrt{I}}, \tag{16}$$

where $b^{(1)}_{k,i}$, $b^{(2)}_{k,i}$, $b^{(1)}_{c,a}$, $b^{(2)}_{c,a}$, $b^{(3)}_{c,a}$, $c^{(1)}_{c,a}$, and $c^{(2)}_{c,a}$ are adjustable parameters, which are determined by fitting AIOMFAC activity coefficients to experimental data sets. The

parameter $b^{(3)}_{c,a}$ was found to describe most aqueous salt solutions when assuming a fixed value of 0.8 $\mathrm{kg}^{1/2}\,\mathrm{mol}^{-1/2}$. In cases where this value did not result in a satisfactory data fit, $b^{(3)}_{c,a}$ was allowed to vary. The parameter $b^{(3)}_{k,i}$ was fixed for all mixed organic–inorganic solutions assuming a value of 1.2 $\mathrm{kg}^{1/2}\,\mathrm{mol}^{-1/2}$. All interaction coefficients in the MR part are symmetric, i.e. $B_{c,a}(I)=B_{a,c}(I)$.

The MR activity coefficients are obtained by differentiating Eq. (13) with respect to the number of moles of solvent main groups, cations, and anions respectively. For a specific solvent main group $k^{\star}$ the related expression is:

$$
\begin{aligned}
\ln \gamma^{\mathrm{MR,(x)}}_{k^{\star}} = & \sum_i B_{k^{\star},i}(I) m_i - \frac{M_{k^{\star}}}{M_{av}} \sum_k \sum_i \left[B_{k,i}(I) + I B'_{k,i}(I) \right] x'_k m_i \\
& - M_{k^{\star}} \sum_c \sum_a \left[B_{c,a}(I) + I B'_{c,a}(I) \right] m_c m_a \\
& - M_{k^{\star}} \sum_c \sum_a \left[2\, C_{c,a}(I) + I C'_{c,a}(I) \right] m_c m_a \sum_i m_i |z_i| \\
& - M_{k^{\star}} \sum_c \sum_{c' \geq c} R_{c,c'}\, m_c m_{c'} \\
& - M_{k^{\star}} \sum_c \sum_{c' \geq c} \sum_a 2\, Q_{c,c',a}\, m_c m_{c'} m_a ,
\end{aligned}
\tag{17}
$$

where m_i, m_c, m_a are the molalities of ions, cations, and anions respectively, x'_k are the salt-free mole fractions of solvent main groups k, and $M_{av}=\sum_s x'_s M_s$ is the average molar mass of the solvent mixture. $M^{\star}_k$ is the molar mass of main group $k^{\star}$, calculated from the molar masses of the corresponding subgroups and their partial contributions to $k^{\star}$. $B'_{k,i}(I)$, $B'_{c,a}(I)$ ($\mathrm{kg}^2\,\mathrm{mol}^{-2}$), and $C'_{c,a}(I)$ ($\mathrm{kg}^3\,\mathrm{mol}^{-3}$) are the partial derivatives with respect to I, e.g. $B'_{c,a}(I)=\partial B'_{c,a}(I)/\partial I$.

The activity coefficient of solvent compound s is then obtained from the main group

contributions by:

$$\ln \gamma_s^{\mathrm{MR,(x)}} = \sum_k \nu_k^{(s)} \ln \gamma_k^{\mathrm{MR,(x)}} \tag{18}$$

where $\nu_k^{(s)}$ refers to the stoichiometric number of main groups k in the solvent molecule s, e.g. $\nu_{\mathrm{CH_n}}^{(1,2-\mathrm{butanediol})}$=4 and $\nu_{\mathrm{OH}}^{(1,2-\mathrm{butanediol})}$=2. In analogy to Eq. (17) the expressions for a specific cation $c^\star$ are:

$$\begin{aligned}
\ln \gamma_{c^\star}^{\mathrm{MR,(x),\infty}} = & \frac{1}{M_{av}} \sum_k B_{k,c^\star}(I) x'_k + \frac{z_{c^\star}^2}{2M_{av}} \sum_k \sum_i B'_{k,i}(I) x'_k m_i \\
& + \sum_a B_{c^\star,a}(I) m_a + \frac{z_{c^\star}^2}{2} \sum_c \sum_a B'_{c,a}(I) m_c m_a \\
& + \sum_a C_{c^\star,a}(I) m_a \sum_i m_i |z_i| \\
& + \sum_c \sum_a \left[C_{c,a}(I) |z_{c^\star}| + C'_{c,a}(I) \frac{z_{c^\star}^2}{2} \sum_i m_i |z_i| \right] m_c m_a \\
& + \sum_c R_{c^\star,c}\, m_c + \sum_c \sum_a Q_{c^\star,c,a}\, m_c m_a,
\end{aligned} \tag{19}$$

and for anion $a^\star$:

$$\begin{aligned}
\ln \gamma_{a^\star}^{\mathrm{MR,(x),\infty}} = & \frac{1}{M_{av}} \sum_k B_{k,a^\star}(I) x'_k + \frac{z_{a^\star}^2}{2M_{av}} \sum_k \sum_i B'_{k,i}(I) x'_k m_i \\
& + \sum_c B_{c,a^\star}(I) m_c + \frac{z_{a^\star}^2}{2} \sum_c \sum_a B'_{c,a}(I) m_c m_a
\end{aligned}$$

$$+ \sum_{c} C_{c,a^{\star}}(I) m_c \sum_{i} m_i |z_i|$$
$$+ \sum_{c} \sum_{a} \left[C_{c,a}(I) |z_{a^{\star}}| + C'_{c,a}(I) \frac{z_{a^{\star}}^2}{2} \sum_{i} m_i |z_i| \right] m_c m_a$$
$$+ \sum_{c} \sum_{c' \geq c} Q_{c,c',a^{\star}} \, m_c m_{c'} . \tag{20}$$

Specific interaction coefficients (and the corresponding fit parameters) between the reference solvent, i.e. water, and the inorganic ions are set to zero ($B_{k=w,i}(I)$=0). Therefore, the unsymmetrical reference state condition for infinite dilution of ions in water ($\gamma_i^{\mathrm{MR}} \rightarrow 1$) is indeed fulfilled and we write $\ln \gamma_{c^{\star}}^{\mathrm{MR},(x),\infty}$ (normalised) instead of $\ln \gamma_{c^{\star}}^{\mathrm{MR},(x)}$. As a consequence of this definition, aqueous electrolyte solutions are described in a similar manner as in a conventional Pitzer model. All binary and ternary coefficients concerning interactions between cations and anions actually describe interactions of cations and anions dissolved in water, thus, including ionic interactions with water. Consequently, specific interaction coefficients between organic functional main groups and ions, the $B_{k,i}(I)$, actually describe the deviations from the interactions of the ions with water. In principle, a different reference solvent could be defined, as discussed in Kiepe et al. (2006), but most tabulated data, e.g. standard chemical potentials, are stated with respect to water as the reference solvent.

2.4 Short-range contribution

The SR contribution G_{SR}^{ex} to the total Gibbs excess energy is represented by the group-contribution method UNIFAC (Fredenslund et al., 1975). The UNIFAC expressions in AIOMFAC include some modifications to better meet the specific properties of atmospheric semi-volatile organics, which typically contain molecules carrying several strongly polar functional groups. Therefore we implemented the more detailed descriptions of alcohol/polyol group interaction parameters published by Marcolli and Peter

(2005). In this way, the relative distances of a molecule's functional groups are taken into account explicitly.

In UNIFAC the activity coefficient γ_j of mixture component j (j used for solute or solvent) is in general expressed as the contributions of a combinatorial part (C), accounting for the geometrical properties of the molecule, and a residual part (R), which reflects inter-molecular interactions:

$$\ln \gamma_j^{\mathrm{SR}} = \ln \gamma_j^C + \ln \gamma_j^R. \tag{21}$$

The expression for the combinatorial part of UNIFAC is (Marcolli and Peter, 2005):

$$\ln \gamma_j^C = \ln \frac{\Phi_j}{x_j} + \frac{z}{2} q_j \ln \frac{\Theta_j}{\Phi_j} + l_j - \frac{\Phi_j}{x_j} \sum_{j'} x_{j'} l_{j'}, \tag{22}$$

where

$$\Phi_j = \frac{r_j x_j}{\sum_{j'} r_{j'} x_{j'}}; \qquad \Theta_j = \frac{q_j x_j}{\sum_{j'} q_{j'} x_{j'}}, \tag{23}$$

with

$$r_j = \sum_t v_t^{(j)} R_t; \qquad q_j = \sum_t v_t^{(j)} Q_t, \tag{24}$$

and

$$l_j = \frac{z}{2}(r_j - q_j) - (r_j - 1). \tag{25}$$

Here, j and j' denote mixture species (solvents or ions), x_j is the mole fraction of component j, and $v_t^{(j)}$ is the number of subgroups of type t in component j. R_t and Q_t are the relative van der Waals subgroup volume and surface area parameters, respectively. The lattice coordination number z, a constant, is set equal to 10 (Fredenslund

et al., 1975). The relative van der Waals subgroup volume and surface area parameters, R_t and Q_t, account for pure component properties. R_t and Q_t values for the ions can be estimated from the ionic radii. However, as Yan et al. (1999) point out, the very small radii of the cations significantly reduce the fitting capabilities of the SR contribution. Therefore we estimated R_t and Q_t values for the ions, taking hydration effects into account, which are especially prominent for the small cations having a high surface charge density. Using an empirical parametrisation, the hydrated group volume and surface area parameters R_t^H and Q_t^H are calculated by (Achard et al., 1994):

$$R_t^H = R_t + N_t^{\mathrm{ADH}} \cdot R_w, \tag{26}$$

$$Q_t^H = Q_t + N_t^{\mathrm{ADH}} \cdot Q_w, \tag{27}$$

where R_w and Q_w refer to the values of the water molecule and N_t^{ADH} are measured apparent dynamic hydration numbers at 303.15 K (Kiriukhin and Collins, 2002). R_t^H and Q_t^H values calculated with this assumptions are listed in Table 1. They are used as constant, ion-specific values over the whole concentration range. In the case of an ionic component, in Eq. (24), R_t and Q_t are replaced by R_t^H and Q_t^H, respectively. The resulting SR contributions were found to be much better suited for an overall model fit compared to unhydrated parameters.

For neutral substances we took the relative subgroup volume and surface area parameters published by Hansen et al. (1991), listed in Table 2. The terms for the residual part of the activity coefficient of j are:

$$\ln \gamma_j^R = \sum_t \nu_t^{(j)} \left[\ln \Gamma_t - \ln \Gamma_t^{(j)} \right], \tag{28}$$

where Γ_t and $\Gamma_t^{(j)}$ are the group residual activity coefficients in the mixture and in a reference solution containing only compound j, a (hypothetical) pure liquid of j, re-

spectively. The expression for the residual activity coefficient of subgroup t is:

$$\ln \Gamma_t = Q_t \left[1 - \ln \left(\sum_m \Theta_m \Psi_{m,t} \right) - \sum_m \left(\frac{\Theta_m \Psi_{t,m}}{\sum_n \Theta_n \Psi_{n,m}} \right) \right] \tag{29}$$

with

$$\Theta_m = \frac{Q_m X_m}{\sum_n Q_n X_n}; \qquad \Psi_{m,n} = e^{-a_{m,n}/T}, \tag{30}$$

where Θ_m is the relative surface area fraction of subgroup m, X_m is the mole fraction of m in the mixture, and $\Psi_{m,n}$ is the temperature dependent function of the subgroup interaction parameter $a_{m,n}$. Note that the subgroup interaction parameters are unsymmetrical, i.e. $a_{m,t} \neq a_{t,m}$. The sums are over all different subgroups. For a more detailed UNIFAC description, we refer to Fredenslund et al. (1975). The subgroup interaction parameters of non-electrolyte solutions have to be estimated using large data sets of binary and higher order mixtures, to distinguish the effective contributions of the different subgroups. In this study, we took the values of $a_{m,n}$ for the alcohol groups and water from the UNIFAC parametrisation of Marcolli and Peter (2005). For LIFAC, Yan et al. (1999) showed, that the model sensitivity to SR interaction parameters $a_{m,n}$ between ions and between ions and organic subgroups is rather small. Thus, in AIOMFAC we set all SR interaction parameters which involve ions to zero, as it is done in LIFAC. This also reduces the number of AIOMFAC fit parameters to those used in the MR part.

Since ions are treated like solvent components in the SR terms, resulting activity coefficients (Eq. 21) are with respect to the symmetrical convention on mole fraction basis. For ions i, the unsymmetrical normalised activity coefficient is determined from:

$$\ln \gamma_i^{\mathrm{SR,(x),\infty}} = \ln \gamma_i^{\mathrm{SR,(x)}} - \ln \gamma_i^{\mathrm{SR,(x),ref}}. \tag{31}$$

The symmetrically normalised value at the reference state is computed from Eqs. (22) and (28) by introducing the reference state conditions of the ions (setting x_w=1, $\sum_s x_s$=0 for $s \neq w$, and $\sum_i x_i$=0):

ACPD
8, 6069–6151, 2008

$$\ln \gamma_i^{\mathrm{SR,(x),ref}} = \ln \frac{r_i}{r_w} + 1 - \frac{r_i}{r_w} + \frac{z}{2} q_i \left[\ln \left(\frac{r_w q_i}{r_i q_w} \right) - 1 + \frac{r_i q_w}{r_w q_i} \right] + q_i \left(1 - \ln \Psi_{w,i} - \Psi_{i,w} \right) \tag{32}$$

where subscript w stands for the reference solvent (water). The last term on the right-hand side of Eq. (32), reflecting the residual part reference contribution, becomes zero as we defined the SR ion-solvent interactions to be zero.

2.5 AIOMFAC activity coefficients

Finally, according to Eqs. (1) and (7), the complete expression for the activity coefficient of solvent species s is:

$$\ln \gamma_s^{(x)} = \ln \gamma_s^{\mathrm{LR,(x)}} + \ln \gamma_s^{\mathrm{MR,(x)}} + \ln \gamma_s^{\mathrm{SR,(x)}} \tag{33}$$

with the specific contributions computed from Eqs. (8), (18), and (21). For the ions, the complete expression with regard to the unsymmetrical convention on molality basis is:

$$\ln \gamma_i^{(m)} = \left[\ln \gamma_i^{\mathrm{LR,(x),\infty}} + \ln \gamma_i^{\mathrm{MR,(x),\infty}} + \ln \gamma_i^{\mathrm{SR,(x),\infty}} \right] - \ln \left[\frac{M_w}{\sum_s x'_s M_s} + M_w \sum_{i'} m_{i'} \right], \tag{34}$$

where M_s is the molar mass of solvent component s, x'_s its salt-free mole fraction, and $m_{i'}$ is the molality of ion i'. The contributions are from Eq. (9) for the LR, Eq. (19) or (20) for the MR (depending on whether i is a cation or an anion), and Eq. (31) for the SR part. The last term on the right-hand side of Eq. (34) converts the activity

coefficient $\ln \gamma_i^{(x),\infty}$ (infinitely diluted reference state on the mole fraction basis) to the activity coefficient on molality basis and infinitely diluted (in water) reference state. This term can be derived using the convention-independence of the chemical potentials ($\mu_i^{(m)}(p,T,n_j)=\mu_i^{(x)}(p,T,n_j)$) and the definitions of the chosen reference states. While a model provides activity coefficients of cations and anions, in experiments one cannot distinguish between the individual interaction contributions of the ions in the mixture. Therefore the mean activity coefficient $\gamma_\pm$ of a salt $M_{\nu^+}X_{\nu^-}$, is defined as:

$$\gamma_\pm = \left[\gamma_+{}^{\nu^+} \cdot \gamma_-{}^{\nu^-}\right]^{1/(\nu^+ + \nu^-)} \tag{35}$$

where ν^+ and ν^-, are the stoichiometric numbers of cations (+) and anions (−) respectively, assuming complete dissociation of the salt. Likewise, using the geometrical mean, the mean molal activity is obtained:

$$\begin{aligned} a_\pm^{(m)} &= \left[\left(a_+^{(m)}\right)^{\nu^+} \cdot \left(a_-^{(m)}\right)^{\nu^-}\right]^{1/(\nu^+ + \nu^-)} \\ &= \left[\left(\frac{m_+}{m^\circ}\gamma_+^{(m)}\right)^{\nu^+} \cdot \left(\frac{m_-}{m^\circ}\gamma_-^{(m)}\right)^{\nu^-}\right]^{1/(\nu^+ + \nu^-)} \\ &= \frac{m_\pm}{m^\circ} \cdot \gamma_\pm^{(m)} \end{aligned} \tag{36}$$

with

$$m_\pm = \left[m_+{}^{\nu^+} \cdot m_-{}^{\nu^-}\right]^{1/(\nu^+ + \nu^-)} . \tag{37}$$

ACPD
8, 6069–6151, 2008

2.6 Estimation of model parameters

The semi-empirical expressions of the MR part contain adjustable parameters, describing interactions between ions, organic functional groups and water. The Debye-Hückel (LR) part and the UNIFAC (SR) part contain no freely adjustable parameters for ions. Organic–organic and organic–water subgroup interactions are parametrized in the SR part. The UNIFAC parameters used here are taken from Marcolli and Peter (2005). Due to the many modifications in the MR part, all pertinent interaction parameters had to be recalculated by fitting the model to experimental data. In a first step, measurements of water activity and mean activity coefficients, comprising several single salt solutions at room temperature, were used to parametrise the inorganic interaction part of the model. In a second step, experimental data of ternary mixtures containing organics (alcohols and polyols), water and inorganic ions were used to fit the specific binary interaction coefficients between ions and organic functional groups. Vapour–liquid equilibria (VLE) data, as well as liquid–liquid equilibria (LLE) compositions, salt solubilities and electromotive force (EMF) measurements were used to establish a broad and reliable database. Subsequently, the two-step procedure to estimate MR parameters is described in more detail.

2.6.1 Step 1: Aqueous inorganic mixtures

In a first step, data sets of binary aqueous salt or inorganic acid solutions were used to fit the MR parameters $b^{(1)}_{c,a}$, $b^{(2)}_{c,a}$, $b^{(3)}_{c,a}$, $c^{(1)}_{c,a}$, and $c^{(2)}_{c,a}$ simultaneously, whereas $b^{(3)}_{c,a}$ was fixed in most cases to a value of $0.8\,\mathrm{kg}^{1/2}\,\mathrm{mol}^{-1/2}$. These MR parameters were determined using the Downhill-Simplex method (Nelder and Mead, 1965) to minimize the following objective function:

$$F = \sum_{d} \sum_{p} w_{d,p} \left[Q^{\mathrm{calc}}_{d,p} - Q^{\mathrm{exp}}_{d,p} \right]^2 \tag{38}$$

where p refers to a specific point in data set d, weighted by factor $w_{d,p}$. The quantity $Q^{\text{calc}}_{d,p}$ represents the calculated and $Q^{\text{exp}}_{d,p}$ the experimentally determined value of a_w or $\gamma_\pm$ at the same mixture composition. Stoichiometric osmotic coefficients (Φ) were converted to water activities by:

$$\ln a_w = -\Phi M_w \sum_i m_i \tag{39}$$

where the sum is over the molality of the ions.

Equilibrium relative humidity (RH) measurements by means of an electrodynamic balance (EDB) can be used to determine water activities of solutions, which are supersaturated with respect to their associated salts. Thus, this method provides data for low RH conditions (low a_w) and is very helpful for model extrapolations to very high ionic strengths (often highly supersaturated). To obtain reasonable model results for such extrapolated conditions, we applied one additional constraint, namely that of a monotonically decreasing a_w with increasing ionic strength (and decreasing x_w) during the minimisation of F. Thermodynamic consistency between different a_w and $\gamma_\pm$ data points of the same mixture can be checked by applying the Gibbs-Duhem relation. As the AIOMFAC expressions satisfy the Gibbs-Duhem relation, plots of modelled and measured a_w and $\gamma_\pm$ disclose disagreements between data sets. On the other hand, a consistent data set of a_w and $\gamma_\pm$ of a mixture can be used to detect model code deficiencies or inconsistencies.

For the aqueous sulphuric acid–ammonium sulphate system, the binary cation–cation interaction parameter $R_{c,c'}$ of (NH_4^+, H^+) and the ternary cation–cation–anion interaction parameter $Q_{c,c',a}$ of (NH_4^+, H^+, HSO_4^-) were determined. For all other systems, these interaction types are not necessary to describe the mixtures and therefore set to zero. The data sets used for parameter estimation and model validation of the considered 28 inorganic substances are referenced in Table 3 and results are discussed in graphical form in Sect. 3.

2.6.2 Step 2: Organic–inorganic mixtures

Given the binary cation–anion MR interactions determined in step 1 and the LR and SR contributions, the organic–inorganic MR interactions were assumed to be responsible for model deviations from measurements for organic–inorganic mixtures. Therefore, in a second step, the MR interaction parameters $b^{(1)}_{k,i}$ and $b^{(2)}_{k,i}$ between solvent main groups k and ions i were fitted using data sets of ternary aqueous organic–inorganic mixtures. In contrast to step 1, where MR parameters of every binary mixture type could be fitted independently, the organic–inorganic interaction parameters are ion specific. Consequently, all ternary mixture data were subjected to a simultaneous fit of $b^{(1)}_{k,i}$ and $b^{(2)}_{k,i}$ to determine ion specific activity coefficients from mixtures containing salts. Although computationally more demanding, the benefit of this model approach is the potential to predict mixtures containing ions and a wide range of organic compounds consisting of the same main groups as the ones used to estimate the parameters. This is one of the fundamental advantages of a group contribution method over substance specific methods. It also shows the need for a wide variety of data involving the same ions and functional groups in different combinations, to assign unambiguously non-idealities of a system to specific organic–inorganic interactions.

In this step, the following case dependent objective function was minimized:

$$F = \sum_d \sum_p \begin{cases} w_{d,p}\left[\frac{Q^{calc}_{d,p} - Q^{exp}_{d,p}}{Q^{exp}_{d,p}}\right]^2 & \text{if: } a_w\text{, VLE, or } \gamma_\pm \text{ data,} \\ w_{d,p}\left[\frac{(a^\alpha_j)_{d,p} - (a^\beta_j)_{d,p}}{0.5\left((a^\alpha_j)_{d,p} + (a^\beta_j)_{d,p}\right)}\right]^2 & \text{if: LLE data,} \\ w_{d,p}\left[(a^{calc}_\pm)_{d,p} - (a^{ref}_\pm)_{d,p}\right]^2 & \text{if: SLE data,} \end{cases} \tag{40}$$

where a^α_j, a^β_j denote the calculated activities of component j in the two liquid phases α

and β. $a_{\pm}^{\mathrm{ref}}$ refers to the calculated mean molal ionic activity of the corresponding salt in a binary saturated aqueous salt solution set as the reference value for comparisons with ternary saturated solutions of the same salt.

VLE data of gas- and liquid-mixture compositions were transformed into activity coefficients of water and the related alcohol for the model fit. Non-ideality of the gas phase was thereby taken into account by applying a fugacity correction (Tsonopoulos, 1974; Zemp and Francesconi, 1992). In LLE, the components exhibit the same activities in coexisting liquid phases. This data type was implemented in the model fit by minimising the relative differences between the activities of the components in the two phases. SLE data was used in a similar way by minimising the difference between mean molal ionic activities ($a_{\pm}$) of the same salt in saturated solutions with different solvent compositions. To provide data of aqueous–polyol–salt solutions, own measurements of water activities at room temperature were performed using an AquaLab water activity meter (Model 3TE, Decagon Devices, USA) with the method described in Marcolli and Peter (2005) and Marcolli and Krieger (2006). The measured water activities are tabulated in Appendix A. EMF data from the literature are commonly listed in terms of molal mean activity coefficients, normalised to the reference state of infinite dilution in the solvent mixture. Because the raw data of EMF measurements was often not obtainable, the listed mean molal activity data was only used for model validation, to check whether the model can reproduce the activity coefficients when the reference state is converted to the mixed solvent case. Data at other temperatures than room temperature, were used with a low weighting factor or just for comparison. Table 4 lists the data sources of ternary alcohol/polyol + water + salt mixtures used for parameter determination and model validation.

Figure 2 shows the binary species combinations, for which the specific MR parameters have been determined so far. Some of the ionic species are of minor importance with respect to their occurrence in atmospheric aerosols, but are helpful to determine unambiguously the individual ionic interaction contributions from salt solution data. Mean interactions between ions and water are indirectly represented by the pa-

rameters of the cation–anion interaction pairs, since the aqueous solution is defined as the reference system as in conventional Pitzer models (Pitzer, 1991). Activities predicted by the AIOMFAC model show significantly larger deviations from measurements for salt-free water–alcohol mixtures than for aqueous electrolyte solutions. This is a consequence and drawback of the group contribution approach of UNIFAC that has to be accepted, if a model should be applicable to a large variety of organic substances.

Since the organic–ion interaction parameters should not compensate for deviations related to inaccuracies in the modelled and measured organic–organic SR (UNIFAC) interactions, the weighting factor for a specific data point was computed as:

$$w_{d,p} = w^{i}_{d,p} \left[x_o(d,p) \sum_i x_i(d,p) \right]^{1/3} \tag{41}$$

where $w^{i}_{d,p}$ is the initial weighting of the data set, x_o the mole fraction of the organic compound, and the sum is over the ions. This empirical formula ensures that those data points are weighted high, which contain large contributions of both, salt and organics. Together with a wide data base, this approach helps to avoid fitting model parameters to other effects than the desired interactions.

3 Results and discussion

3.1 Binary aqueous electrolyte solutions

The AIOMFAC model is aimed at predicting activities in organic–inorganic multicomponent mixtures up to high ionic strength, since the aqueous phase of an aerosol can contain high amounts of inorganic ions. In addition, a well performing inorganic model part is desirable to avoid problems when fitting organic–inorganic interaction parameters. The LIFAC model is only parametrised up to salt saturation and fails to predict activities of supersaturated solutions. For these reasons we redetermined the

MR interaction parameters of AIOMFAC for binary aqueous electrolyte solutions with Eq. (38). The parameters for aqueous solutions of the 28 investigated inorganic electrolyte species are listed in Table 5.

Panels (a) and (b) of Fig. 3 show the AIOMFAC results for water activities and corresponding mean ionic activity coefficients of salts/acids containing the anions Cl^- and Br^-, respectively. Figure 4 gives the analogous presentation for the nitrates and sulphates. The abscissa is mole fraction of the solvent, i.e. water, with respect to completely dissociated salts/acids into cations and anions. Model comparison with the experiments shows in general excellent agreement to very high ionic strengths and low water activities (low RH). Bulk measurements agree very well with each other, whereas measurements in the supersaturated regions show slightly higher variance, likely due to the less accurate experimental methods. The Gibbs-Duhem relation between water activities and the mean activity coefficients is fulfilled for most data sets, since a_w and $\gamma_\pm$ can be fitted accurately using the same model parametrisation as can be seen from the upper and lower figure panels. One exception is $NaNO_3$ which shows incompatible water and mean ionic activities. Here it was decided to follow the water activity data at high concentrations. Deviations from ideal mixing behaviour are higher for the mixtures containing cations with higher surface charge density (e.g. Mg^{2+}, Li^+, H^+) than for mixtures of cations with chaotropic character (e.g. NH_4^+).

Model predictions beyond the concentration range of EDB data are not expected to be important for single-salt aerosol particles since they would effloresce. However, for multi-salt particles, this area maybe of some importance even for subsaturated salt mixtures because the model expressions are based on the ionic strength of the solution. Ternary and higher order mixtures are therefore used to validate the AIOMFAC parametrisation obtained from binary solution data. For example, the ionic strength of aqueous $MgCl_2$ described by EDB measurements ranges up to I=18.4 mol kg^{-1} while EDB measurements of aqueous solutions containing $MgCl_2$+$Mg(NO_3)_2$+$MgSO_4$ with a 1 : 1 : 5 molar ratio range up to I=47.8 mol kg^{-1}. Thus, AIOMFAC needs to describe (extrapolate) aqueous $MgCl_2$ solutions beyond measured binary solutions data. In

the case of aqueous $MgCl_2$, AIOMFAC describes the solution up to I=165.0 mol kg^{-1}. This demonstrates that AIOMFAC can be used up to very high ionic strength and that a thermodynamically reasonable prediction is made, whereas classical extended Debye-Hückel approaches as used in some extended UNIFAC models are applicable only in a range of I<0.1 mol kg^{-1} (Robinson and Stokes, 2002). The concentration range of application of AIOMFAC is comparable to the one of the AIM III model by Clegg et al. (1998b), one of the most commonly used models to calculate activities of aqueous electrolyte solutions at room temperature.

3.2 Activities in multicomponent mixtures

3.2.1 Sulphuric acid–ammonium sulphate mixtures

Sulphuric acid and ammonium sulphate are two of the most common solutes in inorganic aerosols. The dissociation of aqueous sulphuric acid (H_2SO_4) is a two-step process:

$$H_2SO_4 \rightleftharpoons H^+ + HSO_4^-, \quad \text{(R1)}$$

$$HSO_4^- \rightleftharpoons H^+ + SO_4^{2-}. \quad \text{(R2)}$$

The first dissociation step Reaction (R1) has been shown to be essentially complete at atmospheric conditions (Young et al., 1959; Seinfeld and Pandis, 1998). On the other hand, the dissociation Reaction (R2) of the bisulphate ion (HSO_4^-) is strongly temperature dependent and can only be assumed to be complete for very low sulphuric acid concentrations (Young et al., 1959; Dawson et al., 1986; Knopf et al., 2003). In AIOMFAC, the first dissociation step is considered to be complete, the second step is explicitly taken into consideration. This is done by computation of the equilibrium dissociation constant $K_{II}(T)$ with Eq. (42) and iterative adjustment of the ionic molalities until the literature value is met:

$$K_{\mathrm{II}}(T) = \frac{a_{\mathrm{H^+}}(T)\, a_{\mathrm{SO_4^{2-}}}(T)}{a_{\mathrm{HSO_4^-}}(T)} = \frac{m_{\mathrm{H^+}}\, m_{\mathrm{SO_4^{2-}}}\, \gamma_{\mathrm{H^+}}(T)\, \gamma_{\mathrm{SO_4^{2-}}}(T)}{m_{\mathrm{HSO_4^-}}\, \gamma_{\mathrm{HSO_4^-}}(T)}. \tag{42}$$

At 298 K, K_{II}=0.01031 kg mol^{-1} (Knopf et al., 2003). The degree of dissociation, $\alpha_{\mathrm{HSO_4^-}}$, of the $\mathrm{HSO_4^-}$ ion is in general calculated from the molal ratio of actual bisulphate to potential bisulphate amounts:

$$\alpha_{\mathrm{HSO_4^-}} = 1 - \frac{m_{\mathrm{HSO_4^-}}}{m^{\mathrm{max}}_{\mathrm{HSO_4^-}}}, \tag{43}$$

where superscript max indicates the maximum possible molality of bisulphate, when the equilibrium of Reaction (R2) would be completely on the $\mathrm{HSO_4^-}$ side and available $\mathrm{SO_4^{2-}}$ and $\mathrm{H^+}$ (from other sources) would associate to bisulphate:

$$m^{\mathrm{max}}_{\mathrm{HSO_4^-}} = m_{\mathrm{HSO_4^-}} + \min[m_{\mathrm{SO_4^{2-}}}, m_{\mathrm{H^+}}]. \tag{44}$$

For pure aqueous sulphuric acid, $m^{\mathrm{max}}_{\mathrm{HSO_4^-}}$ equals the initial bisulphate molality before dissociation, but in mixtures including other sources for sulphate ions the additional contributions have to be considered. Mixtures of $(\mathrm{NH_4})_2\mathrm{SO_4}$+$\mathrm{H_2SO_4}$+$\mathrm{H_2O}$ contain the following ions: $\mathrm{NH_4^+}$, $\mathrm{SO_4^{2-}}$, $\mathrm{HSO_4^-}$, $\mathrm{H^+}$ (and probably also ions like $\mathrm{NH_4SO_4^-}$). Thus, they include at least 4 binary cation–anion interactions, for which 12 MR parameters have to be fitted simultaneously. At the same time, the equilibrium condition given by Eq. (42) has to be fulfilled. A good description of activities in aqueous sulphuric acid–ammonium sulphate solutions, involving various mixing ratios, was achieved after introducing the additional interaction parameters $R_{\mathrm{NH_4^+,H^+}}$ and $Q_{\mathrm{NH_4^+,H^+,HSO_4^-}}$, listed in Table 6. Water activities as modelled by AIOMFAC are shown in the upper panels of Fig. 5 together with the experimental data used for the model fit. The corresponding degrees of bisulphate dissociation are plotted in the lower panels.

A mixture with $(NH_4)_2SO_4 : H_2SO_4$ ratio of 1:1 corresponds to a solution of NH_4HSO_4 and a 3:1 mixture reflects the composition of letovicite, $(NH_4)_3H(SO_4)_2$. All curves in Fig. 5a) with a mixing ratio of 1:1 or higher are close to or even above the ammonium sulphate a_w curve at the same x_w. This behaviour of the modelled a_w is a consequence of the abscissa scale assuming complete salt and acid dissociation. Panel b) of Fig. 5 shows the same model curves plotted against a x_w-axis taking the modelled partial dissociation of the bisulphate ion into account, while $(NH_4)_2SO_4$ is still assumed to be completely dissociated. With this different scaling, all ternary ammonium sulphate–sulphuric acid mixtures lie in between the curves of pure ammonium sulphate and sulphuric acid. Such scale-effects are in principal expected for the plots of other mixtures too, although perhaps less prominent, depending on the real degree of dissociation of an electrolyte.

3.2.2 Aqueous multi-salt mixtures

The non-ideality of aqueous multi-salt mixtures is in general a result of the interactions between all components. Therefore the AIOMFAC model expressions consider all possible binary cation–anion interactions to compute the overall effect on water and ion activities. Higher order interactions between three or more different ions are neglected, to keep the number of fit parameters low. Figure 6 shows two examples of AIOMFAC water activity predictions. In a) experimental data of an aqueous mixture containing the ions Na^+, NH_4^+, Cl^-, and NO_3^- in a (1:1:1:1) molar ratio are compared with AIOMFAC und ZSR predictions. The ZSR relation (Zdanovskii, 1936, 1948; Stokes and Robinson, 1966) is an expression that can be used to calculate water activities of mixtures based on data from the corresponding binary aqueous salt solutions. The ZSR relation is widely used due to its simple form and generally good performance. For comparison, two ZSR predictions are plotted, assuming that the mixture is a solution of $NaCl+NH_4NO_3$ for ZSR 1 and $NaNO_3+NH_4Cl$ for ZSR 2. Polynomials tabulated in Ha et al. (2000) were used to describe the water activities of binary salt solutions in the recommended a_w range. In the concentration range of the bulk mixture, AIOMFAC

and ZSR 1 are describing the water activity quite well, while ZSR 2 slightly deviates. At supersaturated conditions AIOMFAC and ZSR 1 are still in good agreement with each other and the data, while ZSR 2 overpredicts a_w. EDB data has higher variation than bulk data and AIOMFAC predictions become less accurate at higher concentrations due to the lack of binary data at high ionic strength. This explains the deviations between model and experiments at a_w<0.45 at least partly. One advantage of AIOMFAC, compared with the ZSR relation, is the unambiguous and consistent computation of all mixture component activities – a necessary condition for LLE predictions.

An artificial sea salt mixture was measured and compared to the AIOMFAC prediction as shown in Fig. 6b). The mixture is composed of Na_2SO_4, NaCl, $MgCl_2$, and water with a (salt) molar ratio of (1.000:14.820:1.895) according to the recipe given in Lewis and Schwartz (2004). Again, binary ion combinations like $Mg^{2+}-SO_4^{2-}$ form in the solution and have to be considered in addition to the salts describing the mixture. AIOMFAC a_w predictions and bulk data agree well. As expected from the composition, NaCl dominates the solution's a_w. The generally good performance of AIOMFAC and the ZSR models to predict water activities in multi-salt mixtures shows that binary cation–anion interaction parametrisations seem to be indeed sufficient to describe the mixed solutions, even at supersaturated conditions.

3.3 Alcohol–water–salt mixtures

For the parametrisation of the organic–inorganic MR interactions, a comprehensive compilation of ternary (alcohol+water+salt) data sets were used as described in Sect. 2.6.2. The fitted MR parameters for the calculation of $B_{k,i}(I)$ are listed in Table 7. The inclusion of organic–inorganic MR interaction parameters led to a distinct improvement of the model performance, showing that this type of interactions is indeed important to determine ion and alcohol/polyol activities. In the following, we will present the model performance for selected systems.

Figures 7 and 8 show modelled and measured water activities of polyol–water–ammonium sulphate mixtures. Increase of the salt content decreases the water activity

for a given salt-free mole fraction and may even induce the formation of a liquid–liquid phase separation in case of the longer chain diols. AIOMFAC underestimates the water activity of salt-rich polyol–water mixtures, while it slightly overestimates a_w at moderate and low salt content. The effect of a dissolved salt on the water activity is apparent as the deviation from the salt-free mixture curve. In all cases ammonium sulphate exerts a salting-out effect on the polyols. Note that the MR part of AIOMFAC does not distinguish between 1,2-butanediol and 1,4-butanediol, while the SR part does. Inclusion of organic–inorganic MR parameters leads to an improvement of the water activity predictions by 32–60% for Fig. 7 and 26–73% for Fig. 8.

LLE data is very useful to determine MR parameters for two reasons: (i) the composition measurements of the coexisting phases can be used to compare the activities of the organic compound, of water and of the ions in the two liquid phases simultaneously and (ii) the data is often measured at room temperature. Figure 9 shows a selection of LLE data sets, all containing NaCl as inorganic salt.

Plotted are the relative activity deviations of the components between the two phases:

$$|\text{rel. activity deviation}| = \frac{\left|a_j^\alpha - a_j^\beta\right|}{0.5\left(a_j^\alpha + a_j^\beta\right)} \tag{45}$$

where α, β denote the two different liquid phases. The mean activity coefficient was used in the case of ions. The ions are essentially found in the water rich, polar phase, while the organics are salted-out to the more nonpolar, almost salt-free phase. Good agreement of the activities in the two phases is reached for water, which is present in both phases as a major fraction. The activity deviations of organics and ions are larger, because the model tends to overpredict/underpredict activities when one component is available only in very small amounts in one phase. The introduction of organic–inorganic MR interaction parameters leads to significant improvements of the relative activity deviations ($\Delta a_j^{\alpha,\beta}$) of LLE containing NaCl in the ranges of 4–43% for $\Delta a_w^{\alpha,\beta}$,

93–96% for $\Delta a_o^{\alpha,\beta}$ (where o indicates the organic compound), and 77–94% for $\Delta a_{\pm}^{\alpha,\beta}$. Similar improvements are obtained for LLE systems containing KCl and Na_2SO_4.

VLE data, although often measured at temperatures different from room temperature, offer a useful quality check for salting-out and salting-in effects. To compare AIOMFAC predictions of alcohol and water activity coefficients with VLE measurements, the actual measurement temperatures were used in the SR and LR part of AIOMFAC (without adapting densities and dielectric constants in the LR part). While the MR parametrisation in the present form does not include temperature dependence. Figure 10 shows an example in panel (a) for mixtures of ethanol–water–NaBr. The presence of NaBr increases the activity of ethanol and decreases water activity compared with the salt-free system. If the organic–inorganic interaction parameters were set to zero, the ethanol activity coefficients would show no salting-out effect and instead lie below the dashed curve. This highlights the importance of organic–inorganic interaction parameters for an accurate prediction of gas/particle partitioning. Panel (b) of Fig. 10 shows a rare example of EMF data for the case of a quaternary system containing more than one salt. The published mean activity coefficients are given with respect to the unsymmetrical solvent mixture reference state for ions. Computing the AIOMFAC activity coefficients with respect to this reference state resulted in an excellent agreement with the EMF measurements.

3.4 Comparison with other activity models

In the past, many models were parametrised to compute activity coefficients of either aqueous electrolyte solutions or aqueous organic, electrolyte-free systems. Only a few models combine organic and inorganic approaches to a single framework and only very few of them are aimed at atmospheric aerosol systems. Raatikainen and Laaksonen (2005) showed a comparison of the most established organic–inorganic models suitable for activity calculations of aerosol solutions. One can classify these models into (i) group contribution and (ii) organic substance specific methods. Both model types have

general assets and drawbacks. Group contribution approaches (e.g. extended UNIFAC models) offer the potential to predict activities of a large fraction of organic compounds using parametrisations for only a few functional groups. Substance specific models (e.g. extended UNIQUAC models) in contrast, need individual parametrisations for each organic compound. The accuracy of activity coefficient predictions from organic compound specific models are, as a consequence of the custom-made parametrisation, usually better than the predictions of group contribution models. On the other hand, the compound specific models need experimental data for the parametrisation of every considered mixture and are therefore highly limited in their application compared to group contribution models. In general, these two model types show a trade-off between desired accuracy for specific systems using parametrisations for every compound and desired overall organic–inorganic system application and predictability using a small number of functional group specific parameters. The AIOMFAC model represents a type (i) model. In contrast to most models compared by Raatikainen and Laaksonen (2005), AIOMFAC offers an excellent aqueous electrolyte representation up to high ionic strength. Only the model of Ming and Russell (2002), which includes the AIM model (Clegg et al., 1998a,b) for the inorganic part, yields a comparable accuracy for aqueous electrolyte solutions. Most other models are limited to dilute electrolyte solutions. One disadvantage in this context is the limitation of AIOMFAC to systems at room temperature. The incomplete dissociation of bisulphate in aqueous sulphuric acid–ammonium sulphate systems is explicitly considered in AIOMFAC, other group contribution models, besides the Ming and Russell model, assume always complete bisulphate dissociation or do not implement the related ions at all. Another advantage of AIOMFAC is the consistent model design, able to predict VLE, LLE, and SLE with the same parametrisation. As Raatikainen and Laaksonen pointed out, this is not the case for some models considered in their comparison (e.g. LIFAC). Recently, an improved and modified version of LIFAC (mod. LIFAC) has been published by Kiepe et al. (2006), that is able to predict VLE and LLE. In contrast to AIOMFAC, which has been parametrised using a variety of data types, including LLE and SLE data, organic–

inorganic MR interaction parameters of mod. LIFAC have been obtained from VLE, osmotic coefficients, and mean ionic activity coefficient data.

To describe ion induced liquid-liquid phase separations, models have to explicitly treat interactions between ions and organics. The occurrence of such phase separations has consequences for the gas/particle partitioning of atmospheric aerosols, because in the case of two liquid phases, partitioning of semi-volatile organics to the particulate phase is enhanced compared with the situation of particles consisting of one liquid phase (Erdakos and Pankow, 2004). This increases the amount of particle bound organic mass and decreases the gas phase fraction of semi-volatile components.

AIOMFAC shares the advantage of an explicit organic–inorganic MR interaction part with other models based on LIQUAC/LIFAC, e.g. with the X-UNIFAC models (Erdakos et al., 2006; Chang and Pankow, 2006). In contrast to the other models with a UNIFAC part, AIOMFAC includes the new UNIFAC parametrisation by Marcolli and Peter (2005), which represents the SR contribution of alcohols/polyols better. Methods based on ZSR mixing rules are comparably accurate in predicting water activities of mixtures, but do not consistently predict activity coefficients of all mixture components and can become ambiguous in multi-salt solutions.

Figure 11 shows experimental water activity data of four different aqueous electrolyte solutions at 298 K and corresponding model calculations of AIM III (Aerosol Inorganics Model, http://mae.ucdavis.edu/~sclegg/aim.html) (Clegg et al., 1998b), mod. LIFAC, and AIOMFAC. Panels (a), (b), and (c) of Fig. 11 show that the water activity differences between AIM III and AIOMFAC are in good agreement up to high salt concentrations (a_w<0.6). The experimental data at very high concentrations (a_w<0.45) in panels (a) and (b) indicate the formation of a solid salt (or hydrate) out of the supersaturated solution. This is not reproduced by the models as the formation of solids was not enabled in the model calculations. Panels (a) and (d) show the comparison of mod. LIFAC with AIOMFAC. At low and moderate concentrations the calculated water activities of both models agree well with each other and the measurements. At high salt concentrations mod. LIFAC strongly deviates from AIOMFAC and shows in (a) a steep a_w

increase and in (d) an increase followed by a sharp decrease, features that have to be rated as artefacts of the mod. LIFAC parametrisation. Panel (d) also suggests that for the $Ca(NO_3)_2$ parametrisation in mod. LIFAC only water activity data of bulk measurements were used. The smooth AIOMFAC curves show that the use of EMF data covering high solution concentrations and measurements of ternary mixtures as well as a reasonable constraint on the a_w curve gradient enable much better descriptions and predictions up to high concentrations.

The similarity of mod. LIFAC and AIOMFAC facilitates the comparison between the two models as the AIOMFAC framework can be easily adapted to the model equations and parameters given by Kiepe et al. (2006). Figures 12 and 13 show comparisons between the two models for ternary alcohol/polyol–water–salt mixtures. Panels (a) and (b) of Fig. 12 show two examples of VLE activity coefficient comparisons between mod. LIFAC and AIOMFAC. The agreement of both models with experimental VLE data is overall similar. However, panels (c) and (d) of Fig. 12 show that AIOMFAC represents polyol–water–salt mixtures much better than mod. LIFAC. There the use of further data types besides VLE for the model parametrisations are crucial. Figure 13 shows for four different LLE systems that the AIOMFAC calculations are much more accurate than mod. LIFAC for all LLE datasets. Particularly mean molal activities of the salts in the coexisting phases show large deviations when calculated with mod. LIFAC, which indicates that mod. LIFAC will not be able to predict LLE accurately. These examples show the importance of a wide database covering different experimental methods and data types as well as different organic compounds containing the same functional groups to parametrise an activity model over a wide composition range.

4 Conclusions

AIOMFAC, a semi-empirical group contribution model for computing activity coefficients of organic–inorganic solutions was presented. The thermodynamic framework of AIOMFAC considers explicitly the different Gibbs excess contributions from long-,

middle-, and short-range interactions between all mixture species. Water as the fixed reference solvent for inorganic ions allows the prediction and description of multicomponent LLE, VLE, SLE, and EMF data within the same model. Seven cations, five anions and two organic functional groups, the alkane and the hydroxyl group, were considered using a total of over 150 different data sets. The determination of 28 cation–anion and 18 organic main group–ion interaction parameters in the middle-range part led to a good overall description of mixed alcohol/polyol–water–salt systems. Aqueous electrolyte solutions are predicted very well within the range of available data including high supersaturations. In compliance with the Gibbs-Duhem relation, consistency between mean ionic activity coefficients and water activity predictions was assured. Aqueous mixtures of salts are well predicted by only considering binary cation–anion interaction parameters. Ternary alcohol–water–salt mixtures are described with good agreement to experiments. Although in some cases the data could be more accurately predicted by an organic substance specific model, the group contribution approach offers much more flexibility with a manageable number of groups/species. In principle, the model allows also the calculation of substance specific mixtures if a high accuracy for a specific system is needed. Since other inorganic salts are easily implemented, AIOMFAC is not restricted to atmospheric systems and could be applied in other research fields as well.

In this study we have shown the proof of concept of our model approach. In future, we will extend the AIOMFAC parametrisation to further functional groups and apply it to predict the stable phases and thermodynamic behaviour for multicomponent mixtures of atmospheric relevance. However, for an extension to further functional groups, more experimental data of ternary and higher order organic–inorganic mixtures are often requested.

Appendix A

Tables A1–A9 show data of own water activity measurements at room temperature using an AquaLab water activity meter (Model 3TE, Decagon Devices, USA) for bulk measurements. The experimental method is described in Marcolli and Peter (2005) and Marcolli and Krieger (2006). EDB measurements were performed with the technique described in Colberg et al. (2004).

Acknowledgements. This work was supported by the Swiss National Foundation under project No. 200020-103651. We would like to thank A. A. Zardini and U. K. Krieger of our group, for conducting helpful EDB measurements.

References

Achard, C., Dussap, C. G., and Gros, J. B.: Representation of vapor–liquid-equilibria in water-alcohol electrolyte mixtures with a modified UNIFAC group-contribution method, Fluid Phase Equilibr., 98, 71–89, 1994. 6085, 6114

Bathrick, E.: Precipitation of salts, J. Phys. Chem., 1, 157–169, 1896. 6123

Brenner, D. K., Anderson, E. W., Lynn, S., and Prausnitz, J. M.: Liquid-liquid equilibria for saturated aqueous-solutions of sodium-sulfate plus 1-propanol, 2-propanol, or 2-methylpropan-2-ol, J. Chem. Eng. Data, 37, 419–422, 1992. 6122

Burns, J. A. and Furter, W. F.: Thermodynamic behavior of electrolytes in mixed solvents, a symposium: 170th meeting of the American Chemical Society, Chicago, American Chemical Society, Washington, 99–127, 1975. 6123

Carslaw, K. S., Clegg, S. L., and Brimblecombe, P.: A Thermodynamic Model of the System HCl-HNO_3-H_2SO_4-H_2O, Including Solubilities of HBr, from <200 to 328 K, J. Phys. Chem., 99, 11 557–11 574, 1995. 6072

Chan, C. K., Flagan, R. C., and Seinfeld, J. H.: Water activities of $NH_4NO_3/(NH_4)_2SO_4$ solutions, Atoms. Environ., 26, 1661–1673, 1992. 6118, 6142

Chan, C. K., Ha, Z. Y., and Choi, M. Y.: Study of water activities of aerosols of mixtures of sodium and magnesium salts, Atmos. Environ., 34, 4795–4803, 2000. 6120

Chang, E. I. and Pankow, J. F.: Prediction of activity coefficients in liquid aerosol particles containing organic compounds, dissolved inorganic salts, and water – Part 2: Consideration of phase separation effects by an X-UNIFAC model, Atmos. Environ., 40, 6422–6436, doi: 10.1016/j.atmosenv.2006.04.031, 2006. 6071, 6102

Chou, T. J., Tanioka, A., and Tseng, H. C.: Salting effect on the liquid-liquid equilibria for the partially miscible systems of n-propanol-water and i-propanol-water, Ind. Eng. Chem. Res., 37, 2039–2044, 1998. 6121, 6122, 6147, 6151

Clegg, S. L., Ho, S. S., Chan, C. K., and Brimblecombe, P.: Thermodynamic properties of aqueous $(NH_4)_2SO_4$ to high supersaturation as a function of temperature, J. Chem. Eng. Data, 40, 1079–1090, 1995. 6118, 6142, 6143

Clegg, S. L., Milioto, S., and Palmer, D. A.: Osmotic and Activity Coefficients of Aqueous $(NH_4)_2SO_4$ as a Function of Temperature, and Aqueous $(NH_4)_2SO_4$-H_2SO_4 Mixtures at 298.15 K and 323.15 K, J. Chem. Eng. Data, 41, 455–467, 1996. 6119

Clegg, S. L., Brimblecombe, P., and Wexler, A. S.: Thermodynamic model of the system H^+–NH_4^+–SO_4^{2-}–NO_3^-–H_2O at tropospheric temperatures, J. Phys. Chem. A, 102, 2137–2154, 1998a. 6072, 6101

Clegg, S. L., Brimblecombe, P., and Wexler, A. S.: Thermodynamic model of the system H^+-NH_4^+-Na^+-SO_4^{2-}-NO_3^--Cl^--H_2O at 298.15 K, J. Phys. Chem. A, 102, 2155–2171, 1998b. 6095, 6101, 6102, 6149

Colberg, C. A., Krieger, U. K., and Peter, T.: Morphological investigations of single levitated $H_2SO_4/NH_3/H_2O$ aerosol particles during deliquescence/efflorescence experiments, J. Phys. Chem. A, 108, 2700–2709, doi:10.1021/jp037628r, 2004. 6105

Covington, A. K. and Irish, D. E.: Osmotic and activity-coefficients of aqueous ammonium bromide solutions at 25 degrees C, J. Chem. Eng. Data, 17, 175, 1972. 6118, 6141

Dawson, B. S. W., Irish, D. E., and Toogood, G. E.: Vibrational spectral studies of solutions at elevated-temperatures and pressures. 8. A raman spectral study of ammonium hydrogen sulfate-solutions and the HSO_4^--SO_4^{2-} equilibrium, J. Phys. Chem., 90, 334–341, 1986. 6095, 6119, 6143

De Santis, R., Marrelli, L., and Muscetta, P. N.: Liquid-liquid equilibria in water-aliphatic alcohol systems in the presence of sodium chloride, Chem. Eng. J., 11, 207–214, 1976. 6121, 6122

Debye, P. and Hückel, E.: Zur Theorie der Elektrolyte, Physikalische Zeitschrift, 24, 185–206,

1923. 6077
Decesari, S., Facchini, M. C., Fuzzi, S., and Tagliavini, E.: Characterization of water-soluble organic compounds in atmospheric aerosol: A new approach, J. Geophys. Res. Atmos., 105, 1481–1489, doi:10.1029/1999JD900950, 2000. 6071
Deyhimi, F., Ghalami-Choobar, B., and Salamat-Ahangari, R.: Activity coefficients for NH_4Cl in ethanol-water mixed solvents by electromotive force measurements, J. Mol. Liq., 116, 93–97, 2005. 6123
Dinane, A.: Thermodynamic properties of (NaCl plus KCl+LiCl+H_2O) at T=298.15 K: Water activities, osmotic and activity coefficients, J. Chem. Thermodyn., 39, 96–103, doi:10.1016/j.jct.2006.05.011, 2007. 6120
Erdakos, G. B. and Pankow, J. F.: Gas/particle partitioning of neutral and ionizing compounds to single- and multi-phase aerosol particles. 2. Phase separation in liquid particulate matter containing both polar and low-polarity organic compounds, Atmos. Environ., 38, 1005–1013, doi:10.1016/j.atmosenv.2003.10.038, 2004. 6071, 6102
Erdakos, G. B., Chang, E. I., Pankow, J. F., and Seinfeld, J. H.: Prediction of activity coefficients in liquid aerosol particles containing organic compounds, dissolved inorganic salts, and water – Part 3: Organic compounds, water, and ionic constituents by consideration of short-, mid-, and long-range effects using X-UNIFAC.3, Atmos. Environ., 40, 6437–6452, doi:10.1016/j.atmosenv.2006.04.001, 2006. 6076, 6102
Esteso, M. A., Gonzalez-Diaz, O. M., Hernandez-Luis, F. F., and Fernandez-Merida, L.: Activity-coefficients for NaCl in ethanol-water mixtures at 25°C, J. Solution Chem., 18, 277–288, 1989. 6121
Farelo, F., Lopes, A., and Ferra, M. I. A.: Activity coefficients of potassium chloride and sodium chloride in the quaternary system KCl-NaCl-water-ethanol, J. Solution Chem., 31, 845–860, 2002. 6121, 6148
Fowler, R. H. and Guggenheim, E. A.: Statistical Thermodynamics, Cambridge University Press, UK, 2nd edn., 1949. 6077
Fox, J. J. and Gauge, A. J. H.: The solubility of potassium sulphate in concentrated aqueous solutions of non-electrolytes, J. Chem. Soc., 97, 377–385, 1910. 6123
Fredenslund, A., Jones, R. L., and Prausnitz, J. M.: Group-Contribution Estimation of Activity Coefficients in Nonideal Liquid Mixtures, AIChE J., 21, 1086–1099, 1975. 6072, 6083, 6084, 6086
Gomis, V., Ruiz, F., Devera, G., Lopez, E., and Saquete, M. D.: Liquid–liquid–solid equilibria for

the ternary-systems water sodium-chloride or potassium-chloride 1-propanol or 2-propanol, Fluid Phase Equilibr., 98, 141–147, 1994. 6121, 6147

Gomis, V., Ruiz, F., Asensi, J. C., and Saquete, M. D.: Liquid-liquid-solid equilibria for the ternary systems butanols plus water plus sodium chloride or plus potassium chloride, J. Chem. Eng. Data, 41, 188–191, 1996. 6121, 6122, 6123, 6147, 6151

Guendouzi, M. E., Dinane, A., and Mounir, A.: Water activities, osmotic and activity coefficients in aqueous chloride solutions at T=298.15 K by the hygrometric method, J. Chem. Thermodyn., 33, 1059–1072, 2001. 6119, 6141

Guendouzi, M. E., Mounir, A., and Dinane, A.: Water activity, osmotic and activity coefficients of aqueous solutions of Li_2SO_4, Na_2SO_4, K_2SO_4, $(NH_4)_2SO_4$, $MgSO_4$, $MnSO_4$, $NiSO_4$, $CuSO_4$, and $ZnSO_4$ at T=298.15 K, J. Chem. Thermodyn., 35, 209–220, 2003. 6118, 6142

Ha, Z. Y. and Chan, C. K.: The water activities of $MgCl_2$, $Mg(NO_3)_2$, $MgSO_4$, and their mixtures, Aerosol Sci. Technol., 31, 154–169, 1999. 6118, 6119, 6141, 6142

Ha, Z. Y., Choy, L., and Chan, C. K.: Study of water activities of supersaturated aerosols of sodium and ammonium salts, J. Geophys. Res. Atmos., 105, 11 699–11 709, 2000. 6097, 6117, 6118, 6120, 6141, 6142, 6144, 6149

Hamer, W. J. and Wu, Y.: Osmotic coefficients and mean activity coefficients of uni-univalent electrolytes in water at 25°C, J. Phys. Chem. Ref. Data, 1, 1047–1099, 1972. 6116, 6117, 6118, 6141, 6142

Hansen, H. K., Rasmussen, P., Fredenslund, A., Schiller, M., and Gmehling, J.: Vapor–liquid-equilibria by UNIFAC group contribution. 5. Revision and extension, Ind. Eng. Chem. Res., 30, 2352–2355, 1991. 6085

Heyrovska, R.: Ionic concentrations and hydration numbers of "supporting electrolytes", Electroanalysis, 18, 351–361, doi:10.1002/elan.200503416, 2006. 6074

Iliuta, M. C., Thomsen, K., and Rasmussen, P.: Extended UNIQUAC model for correlation and prediction of vapour–liquid–solid equilibria in aqueous salt systems containing non-electrolytes. Part A. Methanol-water-salt systems, Chem. Eng. Sci., 55, 2673–2686, 2000. 6077

Irish, D. E. and Chen, H.: Equilibria and proton transfer in bisulfate-sulfate system, J. Phys. Chem., 74, 3796, 1970. 6119, 6143

Johnson, A. I. and Furter, W. F.: Vapor–liquid equilibrium in systems containing dissolved salts, Can. J. Chem. Eng., 43, 356, 1965. 6121, 6122, 6123, 6150

Kanakidou, M., Seinfeld, J. H., Pandis, S. N., Barnes, I., Dentener, F. J., Facchini, M. C.,

Van dingenen, R., Ervens, B., Nenes, A., Nielsen, C. J., Swietlicki, E., Putaud, J. P., Balkanski, Y., Fuzzi, S., Horth, J., Moortgat, G. K., Winterhalter, R., Myhre, C. E. L., Tsigaridis, K., Vignati, E., Stephanou, E. G., and Wilson, J.: Organic aerosol and global climate modelling: a review, Atmos. Chem. Phys., 5, 1053–1123, 2005, http://www.atmos-chem-phys.net/5/1053/2005/. 6071

Kato, M., Sato, T., and Hirata, M.: Measurement of Salt Effect on Vapor–Liquid Equilibria by Bubble and Condensation Point Method, J. Chem. Eng. Jpn., 4, 308–311, 1971. 6124

Kiepe, J., Noll, O., and Gmehling, J.: Modified LIQUAC and modified LIFAC – A further development of electrolyte models for the reliable prediction of phase equilibria with strong electrolytes, Ind. Eng. Chem. Res., 45, 2361– 2373, doi:10.1021/ie0510122, 2006. 6072, 6083, 6101, 6103, 6149

Kim, Y. P., Pun, B. K. L., Chan, C. K., Flagan, R. C., and Seinfeld, J. H.: Determination of water activity in ammonium-sulfate and sulfuric-acid mixtures using levitated single particles, Aerosol Sci. Technol., 20, 275–284, 1994. 6119, 6143

Kiriukhin, M. Y. and Collins, K. D.: Dynamic hydration numbers for biologically important ions, Biophys. Chem., 99, 155–168, 2002. 6085, 6114

Knopf, D. A., Luo, B. P., Krieger, U. K., and Koop, T.: Thermodynamic dissociation constant of the bisulfate ion from Raman and ion interaction modeling studies of aqueous sulfuric acid at low temperatures, J. Phys. Chem. A, 107, 4322–4332, doi:10.1021/jp027775+, 2003. 6080, 6095, 6096, 6116, 6143

Lee, S. H., Murphy, D. M., Thomson, D. S., and Middlebrook, A. M.: Chemical components of single particles measured with Particle Analysis by Laser Mass Spectrometry (PALMS) during the Atlanta SuperSite Project: Focus on organic/sulfate, lead, soot, and mineral particles, J. Geophys. Res. Atmos., 107, 4003, doi:10.1029/2000JD000011, 2002. 6071

Lewis, E. R. and Schwartz, S. E.: Sea Salt Aerosol Production: Mechanism, Methods, Measurements, and Models: a critical review., American Geophysical Union, Washington DC, 47–49, 2004. 6098

Li, J. D., Polka, H. M., and Gmehling, J.: A g(e) model for single and mixed-solvent electrolyte systems. 1. Model and results for strong electrolytes, Fluid Phase Equilibr., 94, 89–114, 1994. 6072, 6077

Li, Z. C., Tang, Y. P., Liu, Y., and Li, Y. G.: Salting effect in partially miscible systems of n-butanol water and butanone water .1. Determination and correlation of liquid-liquid equilibrium data, Fluid Phase Equilibr., 103, 143–153, 1995. 6121, 6123, 6151

Lin, C. L., Lee, L. S., and Tseng, H. C.: Phase-equilibria for propan-1-ol plus water plus sodium-chloride and plus potassium-chloride and propan-2-ol plus water plus lithium-chloride and plus lithium bromide, J. Chem. Eng. Data, 38, 306–309, 1993. 6121, 6122, 6150

Lopes, A., Farelo, F., and Ferra, M. I. A.: Activity coefficients of potassium chloride in water-ethanol mixtures, J. Solution Chem., 28, 117–131, 1999. 6122

Lopes, A., Farelo, F., and Ferra, M. I. A.: Activity coefficients of sodium chloride in water-ethanol mixtures: A comparative study of Pitzer and Pitzer-Simonson models, J. Solution Chem., 30, 757–770, 2001. 6121

Lynn, S., Schiozer, A. L., Jaecksch, W. L., Cos, R., and Prausnitz, J. M.: Recovery of anhydrous Na_2SO_4 from SO_2-scrubbing liquor by extractive crystallization: Liquid-liquid equilibria for aqueous solutions of sodium carbonate, sulfate, and/or sulfite plus acetone, 2-propanol, or tert-butyl alcohol, Ind. Eng. Chem. Res., 35, 4236–4245, 1996. 6122, 6151

Marcolli, C. and Krieger, U. K.: Phase changes during hygroscopic cycles of mixed organic/inorganic model systems of tropospheric aerosols, J. Phys. Chem. A, 110, 1881–1893, doi:10.1021/jp0556759, 2006. 6071, 6092, 6105, 6122, 6123, 6124, 6145, 6146, 6150

Marcolli, C. and Peter, T.: Water activity in polyol/water systems: new UNIFAC parameterization, Atmos. Chem. Phys., 5, 1545–1555, 2005, http://www.atmos-chem-phys.net/5/1545/2005/. 6083, 6084, 6086, 6089, 6092, 6102, 6105

Marcolli, C., Luo, B. P., Peter, T., and Wienhold, F. G.: Internal mixing of the organic aerosol by gas phase diffusion of semivolatile organic compounds, Atmos. Chem. Phys., 4, 2593–2599, 2004, http://www.atmos-chem-phys.net/4/2593/2004/. 6071

Maria, S. F., Russell, L. M., Gilles, M. K., and Myneni, S. C. B.: Organic aerosol growth mechanisms and their climate-forcing implications, Science, 306, 1921–1924, doi:10.1126/science.1103491, 2004. 6071

Meyer, T., Polka, H. M., and Gmehling, J.: Low-pressure isobaric vapor–liquid-equilibria of ethanol water mixtures containing electrolytes, J. Chem. Eng. Data, 36, 340–342, 1991. 6121, 6124

Middlebrook, A. M., Murphy, D. M., and Thomson, D. S.: Observations of organic material in individual marine particles at Cape Grim during the First Aerosol Characterization Experiment (ACE 1), J. Geophys. Res. Atmos., 103, 16 475–16 483, 1998. 6071

Ming, Y. and Russell, L. M.: Thermodynamic equilibrium of organic-electrolyte mixtures in aerosol particles., AIChE J., 48, 1331–1348, 2002. 6101

Miro, A. R. and Gonzalez, J. R. A.: Efecto Salino en los Diagramas de Equilibrio Liquido-Vapor. III. Sistemas n-propanol-agua isopropanol-agua con nitrato calcio, Anales de Fisica y Quimica, 797–802, 1958. 6124

Morrison, J. F., Baker, J. C., Meredith, H. C., Newman, K. E., Walter, T. D., Massie, J. D., Perry, R. L., and Cummings, P. T.: Experimental Measurement of Vapor–Liquid Equilibrium in Alcohol/Water/Salt Systems, J. Chem. Eng. Data, 35, 395–404, 1990. 6121, 6122, 6123, 6148

Murphy, D. M. and Thomson, D. S.: Chemical composition of single aerosol particles at Idaho Hill: Negative ion measurements, J. Geophys. Res. Atmos., 102, 6353–6368, 1997. 6071

Murphy, D. M., Cziczo, D. J., Froyd, K. D., Hudson, P. K., Matthew, B. M., Middlebrook, A. M., Peltier, R. E., Sullivan, A., Thomson, D. S., and Weber, R. J.: Single-particle mass spectrometry of tropospheric aerosol particles, J. Geophys. Res. Atmos., 111, D23S32, doi: 10.1029/2006JD007340, 2006. 6071

Mydlarz, J., Jones, A. G., and Millan, A.: Solubility and density isotherms for potassium sulfate-water-2-propanol, J. Chem. Eng. Data, 34, 124–126, 1989. 6123

Myhre, C. E. L., Christensen, D. H., Nicolaisen, F. M., and Nielsen, C. J.: Spectroscopic study of aqueous H_2SO_4 at different temperatures and compositions: Variations in dissociation and optical properties, J. Phys. Chem. A, 107, 1979–1991, doi:10.1021/jp026576n, 2003. 6116, 6143

Nelder, J. A. and Mead, R.: A simplex-method for function minimization, Comput. J., 7, 308–313, 1965. 6089

Pena, M. P., Vercher, E., and Martinez-Andreu, A.: Isobaric vapor–liquid equilibrium for ethanol plus water plus sodium nitrate, J. Chem. Eng. Data, 41, 1097–1100, 1996. 6122

Pinho, S. P. and Macedo, E. A.: Representation of salt solubility in mixed solvents: A comparison of thermodynamic models, Fluid Phase Equilibr., 116, 209–216, 1996. 6121

Pitzer, K. S.: Activity Coefficients in Electrolyte Solutions, CRC Press, Roca Raton, FL, USA, 1991. 6072, 6076, 6077, 6093

Polka, H. M. and Gmehling, J.: Effect of calcium nitrate on the vapor–liquid-equilibria of ethanol plus water and 2-propanol plus water, J. Chem. Eng. Data, 39, 621–624, 1994. 6124

Raatikainen, T. and Laaksonen, A.: Application of several activity coefficient models to water-organic-electrolyte aerosols of atmospheric interest, Atmos. Chem. Phys., 5, 2475–2495, 2005, http://www.atmos-chem-phys.net/5/2475/2005/. 6078, 6100, 6101

Rajendran, M., Renganarayanan, S., and Srinivasan, D.: Salt effect in phase-equilibria and heat of mixing - effect of dissolved inorganic salts on the liquid-liquid equilibria of ethyl-acetate 2-propanol water-system and the vapor–liquid-equilibria and heat of mixing of its constituent binaries, Fluid Phase Equilibr., 70, 65–106, 1991. 6121, 6124

Rieder, R. M. and Thompson, A. R.: Salt effect in vapor–liquid equilibria - ethanol-water saturated with potassium nitrate, Ind. Eng. Chem., 42, 379–382, 1950. 6123

Robinson, R. A. and Stokes, R. H.: Electrolyte Solutions, Dover Publications Inc., New York, USA, 2nd, revised edn., 2002. 6095, 6116, 6117, 6118, 6119, 6141, 6142, 6143, 6149

Rogge, W. F., Mazurek, M. A., Hildemann, L. M., Cass, G. R., and Simoneit, B. R. T.: Quantification of Urban Organic Aerosols at a Molecular Level Identification, Abundance and Seasonal Variation, Atmos. Environ., 27, 1309–1330, 1993. 6071

Rudakoff, G., Hahn, R., and Decker, U.: Calculation of activity-coefficients in ternary-systems with nonvolatile components from measurements of total vapor-pressure, Z. Chem., 12, 467–470, 1972. 6121

Sada, E., Morisue, T., and Miyahara, K.: Salt effects on vapor–liquid equilibrium of isopropanol-water system, J. Chem. Eng. Jpn., 8, 196–201, 1975. 6121, 6124

Seinfeld, J. H. and Pandis, S. N.: Atmospheric Chemistry and Physics: From Air Pollution to Climate Change, J. Wiley & Sons, New York, USA, 1998. 6095

Spann, J. F.: PhD Thesis, Ph.D. thesis, Fayetteville, 1984. 6119, 6143

Staples, B. R.: Activity and Osmotic Coefficients of Aqueous Sulfuric Acid at 298.15 K, J. Phys. Chem. Ref. Data, 10, 779–798, doi:10.1063/1.555648, 1981. 6116, 6143

Stokes, R. H. and Robinson, R. A.: Interactions in aqueous nonelectrolyte solutions .i. Solute-solvent equilibria., J. Phys. Chem., 70, 2126–2130, 1966. 6073, 6097

Taboada, M. E., Veliz, D. M., Galleguillos, H. R., and Graber, T. A.: Solubilities, densities, viscosities, electrical conductivities, and refractive indices of saturated solutions of potassium sulfate in water plus 1-propanol at 298.15, 308.15, and 318.15 K, J. Chem. Eng. Data, 47, 1193–1196, 2002. 6123

Tang, I. N.: Thermodynamic and optical properties of mixed-salt aerosols of atmospheric importance, J. Geophys. Res. Atmos., 102, 1883–1893, 1997. 6117, 6141

Tang, I. N. and Munkelwitz, H. R.: Aerosol Growth Studies – III. Ammonium bisulfate aerosols in a moist atmosphere, J. Aerosol Sci., 8, 321–330, 1977. 6119, 6143

Tang, I. N. and Munkelwitz, H. R.: Water activities, densities, and refractive-indexes of aqueous sulfates and sodium-nitrate droplets of atmospheric importance, J. Geophys. Res. Atmos.,

99, 18 801–18 808, 1994. 6117, 6118, 6119, 6120, 6142, 6143
Taylor, E.: Precipitation of salts, J. Phys. Chem., 1, 718–733, 1896. 6122, 6123
Tsonopoulos, C.: Empirical correlation of second virial-coefficients, AIChE J., 20, 263–272, 1974. 6092
Vener, R. E. and Thompson, A. R.: Solubility and density isotherms for sodium sulfate ethylene glycol water, Ind. Eng. Chem., 41, 2242–2247, 1949. 6122
Vercher, E., Pena, M. P., and Martinezandreu, A.: Isobaric vapor–liquid equilibrium for ethanol plus water plus potassium nitrate., J. Chem. Eng. Data, 41, 66–69, 1996. 6123
Yan, W. D., Topphoff, M., Rose, C., and Gmehling, J.: Prediction of vapor–liquid equilibria in mixed-solvent electrolyte systems using the group contribution concept, Fluid Phase Equilibr., 162, 97–113, 1999. 6072, 6074, 6085, 6086
Young, T. F., Maranville, L. F., and Smith, H. M.: in The Structure of Electrolytic Solutions, Wiley, New York, USA, 1959. 6095, 6119, 6143
Zdanovskii, A. B.: Tr. Solyanoi Lab. Akad. Nauk SSSR, 5–70, 1936. 6073, 6097
Zdanovskii, A. B.: Novyi metod rascheta rastvorimostei elektrolitov v mnogokomponentny sistema. 1., Zh. Fiz. Khim., 22, 1478–1485, 1948. 6073, 6097
Zemp, R. J. and Francesconi, A. Z.: Salt effect on phase-equilibria by a recirculating still, J. Chem. Eng. Data, 37, 313–316, 1992. 6092

Table 1. Relative van der Waals subgroup volume (R_t^H) and surface area. (Q_t^H) parameters for cations and anions considering dynamic hydration.

Ion	r_c (pm) [a]	N^{ADH} [b]	R_t	Q_t	R_t^H [c]	Q_t^H [c]
H^+	0	1.93	0.00	0.00	1.78	2.70
Li^+	76	0.58	0.07	0.17	0.61	0.99
Na^+	102	0.22	0.18	0.31	0.38	0.62
K^+	138	0.00	0.44	0.58	0.44	0.58
NH_4^+	161	0.00	0.69	0.78	0.69	0.78
Mg^{2+}	72	5.85	0.06	0.16	5.44	8.35
Ca^{2+}	123	2.10	0.31	0.46	2.24	3.40
Cl^-	181	0.00	0.99	0.99	0.99	0.99
Br^-	196	0.00	1.25	1.16	1.25	1.16
NO_3^-	179	0.00	0.95	0.97	0.95	0.97
HSO_4^-	215	0.00	1.65	1.40	1.65	1.40
SO_4^{2-}	215	1.83	1.65	1.40	3.34	3.96

[a] The unhydrated (crystal) radii taken from Kiriukhin and Collins (2002) and for NO_3^- and Br^- from Achard et al. (1994). The radius of bisulphate (HSO_4^-) was assumed to be the same as the one for sulphate (SO_4^{2-}).
[b] The apparent dynamic hydration numbers (N^{ADH}) at 303.15 K and 0.1 M taken from Kiriukhin and Collins (2002). Values of N^{ADH} =0 are assigned to the ions, which act as chaotropes (where dynamic hydration is not significant).
[c] Calculated using Eqs. (26) and (27), respectively.

Table 2. Relative van der Waals subgroup volume (R_t) and surface area (Q_t) parameters for solvent subgroups (Hansen et al., 1991).

Main group k	Subgroup t	R_t	Q_t
CH_n (n = 0, 1, 2, 3)	CH_3	0.9011	0.848
	CH_2	0.6744	0.540
	CH	0.4469	0.228
	C	0.2195	0
OH	OH	1.0000	1.200
H_2O	H_2O	0.9200	1.400

Table 3. Data types, number of data points (N), and references of aqueous inorganic solution data. Binary data was used to fit and ternary to validate the AIOMFAC model at room temperature.

Inorganic solutes	Data type [a]	N [b]	Reference
	binary mixtures (1 salt/acid + water)		
HCl	$\gamma_{\pm}$	29	Robinson and Stokes (2002)
	a_w	23	Robinson and Stokes (2002)
HBr	$\gamma_{\pm}$	22	Robinson and Stokes (2002)
	a_w	17	Robinson and Stokes (2002)
HNO_3	$\gamma_{\pm}$	17	Robinson and Stokes (2002)
	a_w	17	Robinson and Stokes (2002)
H_2SO_4	$\alpha_{HSO_4^-}$	4	Knopf et al. (2003)
	$\alpha_{HSO_4^-}$	11	Myhre et al. (2003)
	a_w	81	Staples (1981)
	a_w	64	Robinson and Stokes (2002)
LiCl	$\gamma_{\pm}$	43	Hamer and Wu (1972)
	$\gamma_{\pm}$	37	Robinson and Stokes (2002)
	a_w	43	Hamer and Wu (1972)
	a_w	37	Robinson and Stokes (2002)
LiBr	$\gamma_{\pm}$	37	Robinson and Stokes (2002)
	$\gamma_{\pm}$	43	Hamer and Wu (1972)
	a_w	37	Robinson and Stokes (2002)
	a_w	43	Hamer and Wu (1972)
$LiNO_3$	$\gamma_{\pm}$	30	Robinson and Stokes (2002)
	$\gamma_{\pm}$	43	Hamer and Wu (1972)
	a_w	30	Robinson and Stokes (2002)
	a_w	43	Hamer and Wu (1972)
$LiSO_4$	$\gamma_{\pm}$	17	Robinson and Stokes (2002)
	a_w	17	Robinson and Stokes (2002)

Table 3. Continued.

Inorganic solutes	Data type [a]	N [b]	Reference
NaCl	$\gamma_{\pm}$	30	Hamer and Wu (1972)
	a_w	35	Robinson and Stokes (2002)
	a_w	30	Hamer and Wu (1972)
	a_w	26	Tang (1997)
	a_w	10	Ha et al. (2000)
NaBr	$\gamma_{\pm}$	32	Hamer and Wu (1972)
	$\gamma_{\pm}$	19	Robinson and Stokes (2002)
	a_w	32	Hamer and Wu (1972)
	a_w	19	Robinson and Stokes (2002)
$NaNO_3$	$\gamma_{\pm}$	34	Hamer and Wu (1972)
	a_w	23	Robinson and Stokes (2002)
	a_w	99	Tang and Munkelwitz (1994)
	a_w	19	Ha et al. (2000)
Na_2SO_4	$\gamma_{\pm}$	19	Robinson and Stokes (2002)
	a_w	19	Robinson and Stokes (2002)
	a_w	68	Tang and Munkelwitz (1994)
KCl	$\gamma_{\pm}$	27	Hamer and Wu (1972)
	$\gamma_{\pm}$	21	Robinson and Stokes (2002)
	a_w	27	Hamer and Wu (1972)
	a_w	20	Robinson and Stokes (2002)
	a_w	24	Tang (1997)
KBr	$\gamma_{\pm}$	28	Hamer and Wu (1972)
	$\gamma_{\pm}$	22	Robinson and Stokes (2002)
	a_w	28	Hamer and Wu (1972)
	a_w	22	Robinson and Stokes (2002)
KNO_3	$\gamma_{\pm}$	24	Hamer and Wu (1972)
	a_w	24	Hamer and Wu (1972)
	a_w	18	Robinson and Stokes (2002)

Table 3. Continued.

Inorganic solutes	Data type [a]	N [b]	Reference
K_2SO_4	$\gamma_\pm$	7	Robinson and Stokes (2002)
	a_w	7	Robinson and Stokes (2002)
NH_4Cl	$\gamma_\pm$	23	Robinson and Stokes (2002)
	$\gamma_\pm$	31	Hamer and Wu (1972)
	a_w	23	Robinson and Stokes (2002)
	a_w	31	Hamer and Wu (1972)
	a_w	54	Ha et al. (2000)
NH_4Br	$\gamma_\pm$	23	Covington and Irish (1972)
	a_w	23	Covington and Irish (1972)
NH_4NO_3	$\gamma_\pm$	37	Robinson and Stokes (2002)
	$\gamma_\pm$	49	Hamer and Wu (1972)
	a_w	37	Robinson and Stokes (2002)
	a_w	49	Hamer and Wu (1972)
	a_w	71	Chan et al. (1992)
$(NH_4)_2SO_4$	$\gamma_\pm$	19	Robinson and Stokes (2002)
	a_w	22	Robinson and Stokes (2002)
	a_w	54	Clegg et al. (1995)
	a_w	18	Tang and Munkelwitz (1994)
$MgCl_2$	$\gamma_\pm$	21	Robinson and Stokes (2002)
	a_w	21	Robinson and Stokes (2002)
	a_w	60	Ha and Chan (1999)
$Mg(NO_3)_2$	$\gamma_\pm$	21	Robinson and Stokes (2002)
	a_w	21	Robinson and Stokes (2002)
	a_w	60	Ha and Chan (1999)
$MgSO_4$	$\gamma_\pm$	17	Robinson and Stokes (2002)
	a_w	16	Guendouzi et al. (2003)
	a_w	17	Robinson and Stokes (2002)
	a_w	62	Ha and Chan (1999)

Table 3. Continued.

Inorganic solutes	Data type [a]	N [b]	Reference
$CaCl_2$	$\gamma_\pm$	23	Robinson and Stokes (2002)
	a_w	31	Robinson and Stokes (2002)
	a_w	14	Guendouzi et al. (2001)
$Ca(NO_3)_2$	$\gamma_\pm$	23	Robinson and Stokes (2002)
	a_w	23	Robinson and Stokes (2002)
ternary and higher multicomponent mixtures [c]			
$NaHSO_4$	a_w	32	Tang and Munkelwitz (1994)
NH_4HSO_4	$\alpha_{HSO_4^-}$	15	Irish and Chen (1970)
$\hat{=}$ $(NH_4)_2SO_4 + H_2SO_4$ [1 : 1]	$\alpha_{HSO_4^-}$	9	Young et al. (1959)
	$\alpha_{HSO_4^-}$	7	Dawson et al. (1986)
	a_w	12	Tang and Munkelwitz (1977)
	a_w	40	Spann (1984)
	a_w	23	Kim et al. (1994)
$(NH_4)_2SO_4 + H_2SO_4$ [1 : 2]	a_w	33	Kim et al. (1994)
$(NH_4)_2SO_4 + H_2SO_4$ [2 : 1]	a_w	12	this study (bulk)
	a_w	33	this study (EDB)
$(NH_4)_3H(SO_4)_2$ [3 : 1]	a_w	9	Tang and Munkelwitz (1994)
$(NH_4)_2SO_4 + H_2SO_4$ [0.4824 : 1]	a_w	36	Clegg et al. (1996)
$(NH_4)_2SO_4 + H_2SO_4$ [1.947 : 1]	a_w	35	Clegg et al. (1996)
$Mg(NO_3)_2 + MgSO_4$ [1 : 1]	a_w	57	Ha and Chan (1999)
$MgCl_2 + MgSO_4$ [1 : 1]	a_w	62	Ha and Chan (1999)
$MgCl_2 + Mg(NO_3)_2$ [1 : 1]	a_w	29	Ha and Chan (1999)
$MgCl_2 + Mg(NO_3)_2$ [3 : 1]	a_w	26	Ha and Chan (1999)
$MgCl_2 + Mg(NO_3)_2$ [1 : 3]	a_w	27	Ha and Chan (1999)
$MgCl_2 + Mg(NO_3)_2 + MgSO_4$ [1 : 1 : 1]	a_w	62	Ha and Chan (1999)
$MgCl_2 + Mg(NO_3)_2 + MgSO_4$ [1 : 1 : 5]	a_w	62	Ha and Chan (1999)

Table 3. Continued.

Inorganic solutes	Data type [a]	N [b]	Reference
$NH_4Cl + (NH_4)_2SO_4$ [1 : 1]	a_w	64	Ha et al. (2000)
$NH_4Cl + NH_4NO_3$ [1 : 1]	a_w	58	Ha et al. (2000)
$NaCl + NH_4Cl$ [1 : 1]	a_w	73	Ha et al. (2000)
$NaCl + NH_4Cl$ [3 : 1]	a_w	73	Ha et al. (2000)
$NaCl + NH_4NO_3$ [1 : 1]	a_w	62	Ha et al. (2000)
	a_w	13	this study (bulk)
$NaCl + NH_4NO_3$ [3 : 1]	a_w	62	Ha et al. (2000)
$NaNO_3 + (NH_4)_2SO_4$ [1 : 1]	a_w	62	Ha et al. (2000)
$NaNO_3 + (NH_4)_2SO_4$ [3 : 1]	a_w	64	Ha et al. (2000)
$NaNO_3 + NH_4NO_3$ [1 : 1]	a_w	61	Ha et al. (2000)
$NaNO_3 + NH_4NO_3$ [3 : 1]	a_w	49	Ha et al. (2000)
$NaNO_3 + Na_2SO_4$ [1 : 1]	a_w	26	Ha et al. (2000)
$NaNO_3 + Na_2SO_4$ [3 : 1]	a_w	26	Ha et al. (2000)
$NaCl + KCl + LiCl$ [1 : 1 : 1]	a_w	19	Dinane (2007)
$NaCl + KCl + LiCl$ [2 : 1 : 1]	a_w	16	Dinane (2007)
$NaCl + KCl + LiCl$ [1 : 2 : 2]	a_w	16	Dinane (2007)
$NaCl + Na_2SO_4 + MgCl_2$ [14.82 : 1.00 : 1.89]	a_w	10	this study (bulk)
$Na_2SO_4 + MgCl_2 + MgSO_4$ [1.49 : 1.00 : 1.26]	a_w	9	this study (bulk)
$NaCl + MgSO_4$ [1 : 1]	a_w	8	this study (bulk)
	a_w	68	Chan et al. (2000)

[a] Water activity (a_w) data was calculated from listed osmotic coefficients and solute molalities when not given in the literature.
[b] Data points by Tang and Munkelwitz (1994) were generated by using the given polynomials to their measurements.
[c] In brackets the molar ratio of the salts or alternatively the ratio of ammonium sulphate to sulphuric acid.

Table 4. Data types, number of data points (N), temperature range, and references of organic–inorganic–water mixtures used to fit or validate the AIOMFAC model.

Salt + alcohol in mixture [a]	Data type [b]	N	T (K) [c]	Reference
LiCl + 2-propanol	VLE	30	348.25	Sada et al. (1975)
	VLE	37	353–357	Lin et al. (1993)
LiBr + ethanol	VLE	19	333.15	Rudakoff et al. (1972)
LiBr + 2-propanol	VLE	21	348.15	Sada et al. (1975)
	VLE	37	353–357	Lin et al. (1993)
NaCl + ethanol	$\gamma_{\pm}$	45	298	Lopes et al. (2001)
	$\gamma_{\pm}$	123	298	Esteso et al. (1989)
	SLE	7	298	Pinho and Macedo (1996)
	VLE	14	316–332	Meyer et al. (1991)
	VLE	16	306–313	Meyer et al. (1991)
	VLE	13	350–361	Johnson and Furter (1965)
NaCl + KCl + ethanol	$\gamma_{\pm}$	31	298	Farelo et al. (2002)
NaCl + 1-propanol	VLE	43	359–363	Morrison et al. (1990)
	VLE	10	362–375	Johnson and Furter (1965)
	VLE	36	360–365	Lin et al. (1993)
	LLE	11	298	De Santis et al. (1976)
	LLE	8	298	Chou et al. (1998)
	LLE	5	298	Gomis et al. (1994)
NaCl + 2-propanol	VLE	56	353–362	Rajendran et al. (1991)
	LLE	8	298	De Santis et al. (1976)
	LLE	5	298	Gomis et al. (1994)
NaCl + 1-butanol	LLE	20	298	De Santis et al. (1976)
	LLE	10	298	Li et al. (1995)
	LLE	19	313.15	De Santis et al. (1976)
NaCl + 2-butanol	LLE	20	298	De Santis et al. (1976)
	LLE	9	298	Gomis et al. (1996)

Table 4. Continued.

Salt + alcohol in mixture [a]	Data type [b]	N	T (K) [c]	Reference
NaCl + isobutanol	LLE	9	298	Gomis et al. (1996)
	LLE	20	298	De Santis et al. (1976)
NaCl + tert-butanol	LLE	14	298	De Santis et al. (1976)
	LLE	8	298	Gomis et al. (1996)
NaCl + glycerol	a_w	10	298	Marcolli and Krieger (2006)
NaCl + 1,4-butanediol	a_w	10	298	Marcolli and Krieger (2006)
NaCl + 1,2-hexanediol	a_w	17	298	Marcolli and Krieger (2006)
NaBr + 1-propanol	VLE	30	360–364	Morrison et al. (1990)
	LLE	11	298	Chou et al. (1998)
NaBr + 2-propanol	VLE	52	353–358	Morrison et al. (1990)
$NaNO_3$ + ethanol	VLE	122	351–373	Pena et al. (1996)
	SLE	10	303.15	Taylor (1896)
Na_2SO_4 + 1,2-ethanediol	SLE	13	308.15	Vener and Thompson (1949)
Na_2SO_4 + 1-propanol	SLE	5	293.15	Brenner et al. (1992)
	LLE	12	297-353	Brenner et al. (1992)
Na_2SO_4 + 2-propanol	SLE	10	293.15	Brenner et al. (1992)
	SLE	11	298	Brenner et al. (1992)
	LLE	8	302–353	Brenner et al. (1992)
	LLE	8	308.15	Lynn et al. (1996)
Na_2SO_4 + tert-butanol	SLE	5	293.15	Brenner et al. (1992)
	LLE	12	308.15	Lynn et al. (1996)
	LLE	13	296–353	Brenner et al. (1992)
KCl + ethanol	VLE	11	350–369	Johnson and Furter (1965)
	$\gamma_\pm$	60	298	Lopes et al. (1999)
KCl + 1-propanol	VLE	8	361–372	Johnson and Furter (1965)
	VLE	40	360–363	Lin et al. (1993)
	LLE	4	298	Gomis et al. (1996)
	LLE	9	298	Chou et al. (1998)

Table 4. Continued.

Salt + alcohol in mixture [a]	Data type [b]	N	T (K) [c]	Reference
KCl + 1-butanol	LLE	8	298	Li et al. (1995)
	LLE	9	298	Gomis et al. (1996)
KCl + 2-butanol	LLE	9	298	Gomis et al. (1996)
KCl + isobutanol	LLE	9	298	Gomis et al. (1996)
KBr + ethanol	VLE	40	354–357	Burns and Furter (1975)
	SLE	11	303.15	Taylor (1896)
KBr + 1-propanol	VLE	36	359–362	Morrison et al. (1990)
KBr + 1-butanol	LLE	10	298	Li et al. (1995)
KNO_3 + ethanol	VLE	13	351–369	Rieder and Thompson (1950)
	VLE	49	351–364	Vercher et al. (1996)
	SLE	10	303.15	Bathrick (1896)
K_2SO_4 + ethanol	SLE	12	298	Fox and Gauge (1910)
K_2SO_4 + 1-propanol	SLE	16	298	Taboada et al. (2002)
K_2SO_4 + 2-propanol	SLE	26	293, 303	Mydlarz et al. (1989)
NH_4Cl + ethanol	VLE	10	350–366	Johnson and Furter (1965)
	$\gamma_\pm$	108	298	Deyhimi et al. (2005)
	SLE	10	303.15	Bathrick (1896)
NH_4Cl + 1-propanol	VLE	9	362–383	Johnson and Furter (1965)
NH_4Br + ethanol	VLE	43	355–358	Burns and Furter (1975)
NH_4NO_3 + glycerol	a_w	9	298	Marcolli and Krieger (2006)
NH_4NO_3 + 1,4-butanediol	a_w	12	298	Marcolli and Krieger (2006)
NH_4NO_3 + 1,2-hexanediol	a_w	16	298	Marcolli and Krieger (2006)
$(NH_4)_2SO_4$ + glycerol	a_w	10	298	Marcolli and Krieger (2006)
$(NH_4)_2SO_4$ + 1,2-butanediol	a_w	8	298	this study (bulk)
$(NH_4)_2SO_4$ + 1,4-butanediol	a_w	12	298	Marcolli and Krieger (2006)

Table 4. Continued.

Salt + alcohol in mixture [a]	Data type [b]	N	T (K) [c]	Reference
$(NH_4)_2SO_4$ + 1,2,4-butanetriol	a_w	9	298	this study (bulk)
$(NH_4)_2SO_4$ + 2,4-pentanediol	a_w	10	298	this study (bulk)
$(NH_4)_2SO_4$ + 1,2-hexanediol	a_w	12	298	Marcolli and Krieger (2006)
$(NH_4)_2SO_4$ + 2,5-hexanediol	a_w	8	298	this study (bulk)
$(NH_4)_2SO_4$ + 1,7-heptanediol	a_w	9	298	this study (bulk)
$CaCl_2$ + ethanol	VLE	13	307–321	Meyer et al. (1991)
$CaCl_2$ + 2-propanol	VLE	21	348.25	Sada et al. (1975)
	VLE	42	356–368	Rajendran et al. (1991)
	VLE	12	354–356	Kato et al. (1971)
$Ca(NO_3)_2$ + ethanol	VLE	42	335–356	Polka and Gmehling (1994)
$Ca(NO_3)_2$ + 1-propanol	VLE	17	362–372	Miro and Gonzalez (1958)
$Ca(NO_3)_2$ + 2-propanol	VLE	23	355–361	Miro and Gonzalez (1958)
	VLE	41	335–354	Polka and Gmehling (1994)

[a] The mixtures contain water in addition to the stated components.
[b] The data types used to fit the model parameters. VLE data was translated into γ_o, γ_w values, where o indicates the organic compound, LLE data into a_w, a_o, $a_\pm$, and SLE data into $a_\pm$ values.
[c] The temperature at which data was measured. For isobaric experiments, the approximate temperature range is shown.

ACPD
8, 6069–6151, 2008

Table 5. Fitted binary cation–anion MR interaction parameters.

c	a	$b^{(1)}_{c,a}$ (kg mol^{-1})	$b^{(2)}_{c,a}$ (kg mol^{-1})	$b^{(3)}_{c,a}$ (kg$^{1/2}$ mol$^{-1/2}$)	$c^{(1)}_{c,a}$ (kg^{2} mol^{-2})	$c^{(2)}_{c,a}$ (kg$^{1/2}$ mol$^{-1/2}$)
H^+	Cl^-	0.182003	0.243340	0.8	0.033319	0.504672
H^+	Br^-	0.120325	0.444859	0.8	0.080767	0.596776
H^+	NO_3^-	0.210638	0.122694	0.8	−0.101736	1.676420
H^+	SO_4^{2-}	0.097108	−0.004307	1.0	0.140598	0.632246
H^+	HSO_4^-	0.313812	−4.895466	1.0	−0.358419	0.807667
Li^+	Cl^-	0.106555	0.206370	0.8	0.053239	0.535548
Li^+	Br^-	0.106384	0.316480	0.8	0.057602	0.464658
Li^+	NO_3^-	0.076313	0.300550	0.8	0.046701	0.664928
Li^+	SO_4^{2-}	0.114470	0.035401	0.8	−0.263258	1.316967
Na^+	Cl^-	0.053741	0.079771	0.8	0.024553	0.562981
Na^+	Br^-	0.180807	0.273114	0.8	−0.506598	2.209050
Na^+	NO_3^-	0.001164	−0.102546	0.410453	0.002535	0.512657
Na^+	SO_4^{2-}	0.001891	−0.424184	0.8	−0.223851	1.053620
Na^+	HSO_4^-	0.021990	0.001863	0.8	0.019921	0.619816
K^+	Cl^-	0.016561	−0.002752	0.8	0.020833	0.670530
K^+	Br^-	0.033688	0.060882	0.8	0.015293	0.565063
K^+	NO_3^-	0.000025	−0.413172	0.357227	−0.000455	0.242244
K^+	SO_4^{2-}	0.004079	−0.869936	0.8	−0.092240	0.918743
NH_4^+	Cl^-	0.001520	0.049074	0.116801	0.011112	0.653256
NH_4^+	Br^-	0.002498	0.081512	0.143621	0.013795	0.728984
NH_4^+	NO_3^-	−0.000057	−0.171746	0.260000	0.005510	0.529762
NH_4^+	SO_4^{2-}	0.000373	−0.906075	0.545109	−0.000379	0.354206
NH_4^+	HSO_4^-	0.009054	0.214405	0.228956	0.017298	0.820465

Table 5. Continued.

c	a	$b^{(1)}_{c,a}$ (kg mol^{-1})	$b^{(2)}_{c,a}$ (kg mol^{-1})	$b^{(3)}_{c,a}$ (kg$^{1/2}$ mol$^{-1/2}$)	$c^{(1)}_{c,a}$ (kg^{2} mol^{-2})	$c^{(2)}_{c,a}$ (kg$^{1/2}$ mol$^{-1/2}$)
Mg^{2+}	Cl^-	0.195909	0.332387	0.8	0.072063	0.397920
Mg^{2+}	NO_3^-	0.430671	0.767242	0.8	−0.511836	1.440940
Mg^{2+}	SO_4^{2-}	0.122364	−3.425876	0.8	−0.738561	0.864380
Ca^{2+}	Cl^-	0.104920	0.866923	0.8	0.072063	0.365747
Ca^{2+}	NO_3^-	0.163282	0.203681	0.8	−0.075452	1.210906

ACPD
8, 6069–6151, 2008

Table 6. Additional aqueous electrolyte interaction parameters $R_{c,c'}$ and $Q_{c,c',a}$ (set to 0.0 if not specified).

c	c'	a	$R_{c,c'}$ (kg mol^{-1})	$Q_{c,c',a}$ (kg^2 mol^{-2})
NH_4^+	H^+		−0.220938	
NH_4^+	H^+	HSO_4^-		0.002414

ACPD
8, 6069–6151, 2008

Table 7. Fitted binary MR parameters of organic–inorganic interactions between the functional main groups CH_n and OH, and the ions.

k	i	$b^{(1)}_{k,i}$ (kg mol^{-1})	$b^{(2)}_{k,i}$ (kg mol^{-1})
CH_n	Li^+	0.242840	0.004770
OH	Li^+	−0.029646	−1.033024
CH_n	Na^+	0.124972	−0.031880
OH	Na^+	0.080254	0.002201
CH_n	K^+	0.121449	0.015499
OH	K^+	0.065219	−0.170779
CH_n	NH_4^+	0.103096	−0.006344
OH	NH_4^+	0.039373	0.001083
CH_n	Ca^{2+}	0.000019	−0.060807
OH	Ca^{2+}	0.839628	−0.765776
CH_n	Cl^-	0.014974	0.142574
OH	Cl^-	−0.042460	−0.128063
CH_n	Br^-	0.000042	−0.025473
OH	Br^-	−0.007153	0.483038
CH_n	NO_3^-	0.018368	0.669086
OH	NO_3^-	−0.128216	−0.962408
CH_n	SO_4^{2-}	0.101044	−0.070253
OH	SO_4^{2-}	−0.164709	0.574638

Table A1. Water activities from bulk measurements of aqueous ammonium sulphate–sulphuric acid mixtures at 298.15 K with a $(NH_4)_2SO_4 : H_2SO_4$ molar ratio of 2 : 1. Concentrations of the electrolytes are given fractions.

Composition of aqueous solutions (mass fractions).		
$(NH_4)_2SO_4$	H_2SO_4	a_w [a]
0.0247	0.0092	0.995
0.0611	0.0227	0.978
0.0977	0.0362	0.966
0.1340	0.0497	0.945
0.1704	0.0633	0.924
0.2068	0.0768	0.900
0.2433	0.0903	0.870
0.2583	0.0958	0.856
0.2733	0.1014	0.843
0.2882	0.1070	0.829
0.3036	0.1127	0.816
0.3181	0.1181	0.799

[a] The accuracy is specified to be ±0.003 a_w.

Table A2. Water activities from EDB measurements of aqueous ammonium sulphate–sulphuric acid mixtures at 298.15 K with a $(NH_4)_2SO_4 : H_2SO_4$ molar ratio of 2 : 1. Concentrations of the electrolytes are given in mass fractions.

Composition of aqueous solutions (mass fractions).		
$(NH_4)_2SO_4$	H_2SO_4	a_w [a]
0.3137	0.1164	0.803
0.3296	0.1223	0.783
0.3398	0.1261	0.770
0.3489	0.1295	0.758
0.3583	0.1330	0.746
0.3678	0.1365	0.733
0.3765	0.1397	0.721
0.3852	0.1430	0.709
0.3940	0.1462	0.697
0.4031	0.1496	0.684
0.4110	0.1526	0.672
0.4206	0.1561	0.659
0.4289	0.1592	0.647
0.4374	0.1623	0.635
0.4468	0.1658	0.622
0.4544	0.1687	0.610
0.4624	0.1716	0.597
0.4718	0.1751	0.585
0.4798	0.1781	0.572
0.4875	0.1809	0.559
0.4955	0.1839	0.547
0.5029	0.1866	0.535
0.5106	0.1895	0.522

ACPD
8, 6069–6151, 2008

TableA2. Continued.

Composition of aqueous solutions (mass fractions).		
$(NH_4)_2SO_4$	H_2SO_4	a_w [a]
0.5193	0.1927	0.510
0.5273	0.1957	0.497
0.5359	0.1989	0.485
0.5434	0.2017	0.473
0.5532	0.2053	0.460
0.5606	0.2081	0.448
0.5697	0.2114	0.435
0.5793	0.2150	0.422
0.5847	0.2170	0.409
0.5930	0.2201	0.396

[a] The accuracy is assumed to be ±0.016 a_w.

Table A3. Bulk water activity measurements of aqueous sodium chloride–ammonium nitrate mixtures at 298.15 K with a NaCl : NH_4NO_3 molar ratio of 1:1.

Composition of aqueous solutions (mass fractions).		
NaCl	NH_4NO_3	a_w [a]
0.0038	0.0052	0.991
0.0093	0.0127	0.985
0.0207	0.0283	0.973
0.0338	0.0462	0.959
0.0456	0.0624	0.946
0.0591	0.0809	0.928
0.0709	0.0971	0.910
0.0844	0.1156	0.891
0.0967	0.1323	0.872
0.1102	0.1508	0.847
0.1220	0.1670	0.824
0.1351	0.1849	0.799
0.1478	0.2022	0.775

[a] The accuracy is specified to be ±0.003 a_w.

Table A4. Bulk water activity measurements of aqueous sodium chloride–magnesium sulphate mixtures at 298.15 K with a NaCl : $MgSO_4$ molar ratio of 1 : 1.

Composition of aqueous solutions (mass fractions).		
NaCl	$MgSO_4$	a_w [a]
0.0088	0.0173	0.989
0.0131	0.0259	0.987
0.0289	0.0571	0.971
0.0404	0.0796	0.956
0.0559	0.1101	0.934
0.0670	0.1320	0.908
0.0828	0.1632	0.865
0.0939	0.1851	0.825

[a] The accuracy is specified to be ±0.003 a_w.

ACPD
8, 6069–6151, 2008

Table A5. Bulk water activity measurements of aqueous "sea salt"-like sodium chloride–sodium sulphate–magnesium chloride mixtures at 298.15 K with a $NaCl:Na_2SO_4:MgCl_2$ molar ratio of 14.820 : 1.000 : 1.895.

Composition of aqueous solutions (mass fractions).			
NaCl	Na_2SO_4	$MgCl_2$	a_w [a]
0.0029	0.0005	0.0006	0.994
0.0102	0.0017	0.0021	0.989
0.0321	0.0053	0.0067	0.975
0.0532	0.0087	0.0111	0.961
0.0743	0.0122	0.0155	0.926
0.0962	0.0158	0.0200	0.913
0.1180	0.0194	0.0246	0.884
0.1399	0.0229	0.0291	0.852
0.1618	0.0265	0.0337	0.814
0.1822	0.0299	0.0380	0.777

[a] The accuracy is specified to be ±0.003 a_w.

Table A6. Bulk water activity measurements of aqueous sodium sulphate–magnesium chloride–magnesium sulphate mixtures at 298.15 K with a $Na_2SO_4 : MgCl_2 : MgSO_4$ molar ratio of 1.490 : 1.000 : 1.263.

Composition of aqueous solutions (mass fractions).			
Na_2SO_4	$MgCl_2$	$MgSO_4$	a_w [a]
0.0037	0.0017	0.0026	0.992
0.0175	0.0079	0.0126	0.987
0.0309	0.0139	0.0222	0.978
0.0438	0.0197	0.0315	0.968
0.0577	0.0259	0.0414	0.955
0.0701	0.0315	0.0503	0.94
0.0849	0.0382	0.0609	0.919
0.0987	0.0444	0.0709	0.895
0.1121	0.0504	0.0805	0.867

[a] The accuracy is specified to be ±0.003 a_w.

ACPD
8, 6069–6151, 2008

Table A7. Bulk water activity measurements of ammonium sulphate–polyol–water mixtures at 298.15 K. Concentrations are given in mass fractions of $(NH_4)_2SO_4$ and polyols.

Composition of aqueous solutions (mass fractions).			
$(NH_4)_2SO_4$	1,2-butanediol	1,2,4-butanetriol	a_w [a]
0.0150	0.7726		0.683
0.0304	0.6613		0.761
0.0797	0.5384		0.780
0.1355	0.4149		0.787
0.1980	0.3142		0.784
0.2821	0.1875		0.787
0.3540	0.0888		0.787
0.4320	0.0000		0.802
0.0158		0.7737	0.531
0.0364		0.6845	0.614
0.0680		0.5961	0.668
0.1055		0.4922	0.716
0.1580		0.3992	0.743
0.2249		0.3030	0.750
0.2966		0.1872	0.769
0.3615		0.0903	0.787
0.4320		0.0000	0.802

[a] The accuracy is specified to be ±0.015 a_w.

Table A8. Bulk water activity measurements of ammonium sulphate–polyol–water mixtures at 298.15 K. Concentrations are given in mass fractions of $(NH_4)_2SO_4$ and polyols.

Composition of aqueous solutions (mass fractions).			
$(NH_4)_2SO_4$	2,4-pentanediol	2,5-hexanediol	a_w [a]
0.0073	0.7051		0.796
0.0461	0.4627		0.846
0.0900	0.3592		0.852
0.1373	0.2649		0.851
0.1971	0.1731		0.851
0.2575	0.1046		0.845
0.3304	0.0507		0.830
0.3608	0.0342		0.820
0.4190	0.0121		0.795
0.4320	0.0000		0.802
0.0433		0.4299	0.883
0.0736		0.3488	0.883
0.1083		0.2654	0.889
0.1480		0.1955	0.882
0.1902		0.1241	0.886
0.2302		0.0725	0.879
0.2911		0.0338	0.867
0.4320		0.0000	0.802

[a] The accuracy is specified to be ±0.015 a_w.

Table A9. Bulk water activity measurements of ammonium sulphate–1,7-heptanediol–water mixtures at 298.15 K. Concentrations are given in mass fractions of $(NH_4)_2SO_4$ and 1,7-heptanediol.

Composition of aqueous solutions (mass fractions).		
$(NH_4)_2SO_4$	1,7-heptanediol	a_w [a]
0.0144	0.4111	0.952
0.0327	0.1983	0.943
0.0477	0.1218	0.946
0.0453	0.0511	0.948
0.0480	0.0536	0.943
0.0765	0.0507	0.941
0.0981	0.0320	0.944
0.1338	0.0160	0.938
0.4320	0.0000	0.802

[a] The accuracy is specified to be ±0.015 a_w.

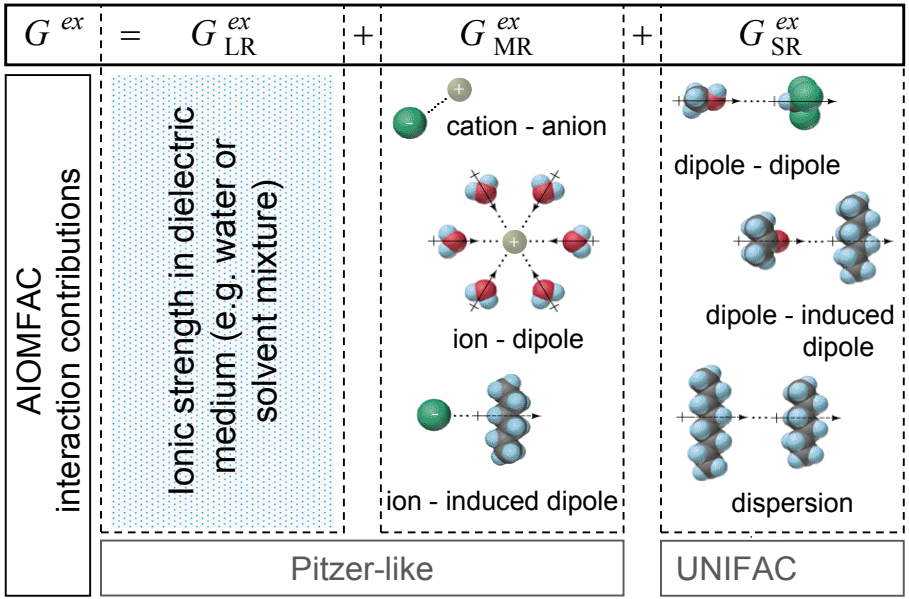

Fig. 1. Three major terms represent different types of molecular interactions in a solution and add up to the excess Gibbs energy (G^{ex}) of a certain system in the AIOMFAC model. Dispersion forces, also called London forces, are present in any mixture and denote induced dipole–induced dipole interactions. Long-range forces between ions are described by only taking the electric charge interactions into account while neglecting other ion specific properties (e.g. the different radii).

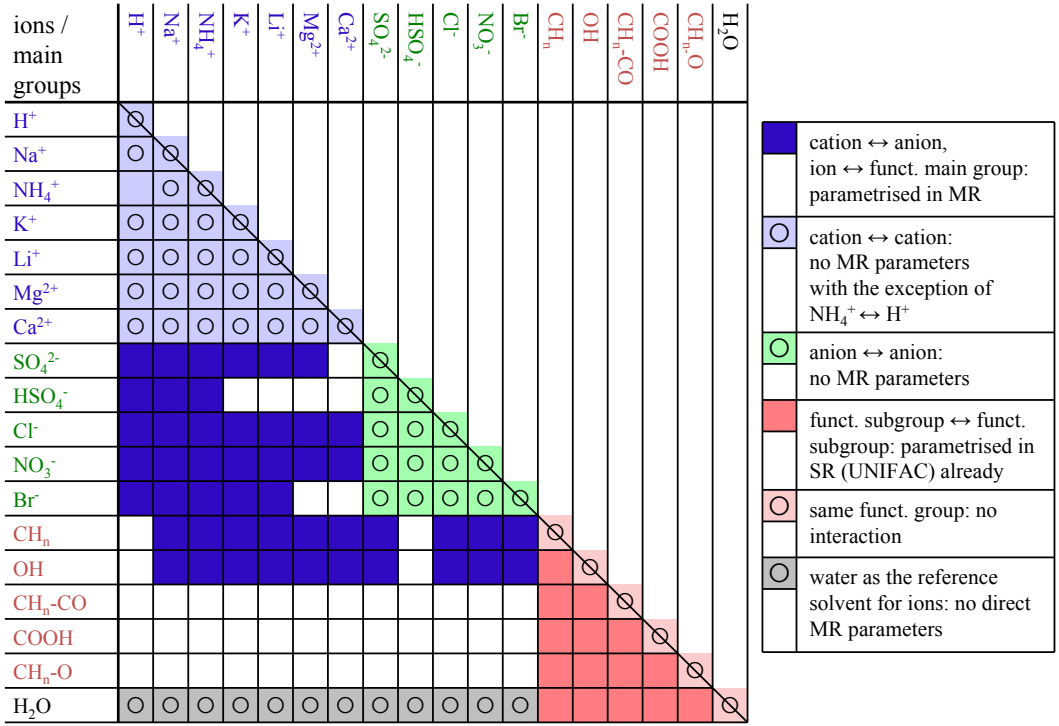

Fig. 2. Scheme of the currently parametrised interactions in the MR and SR part. Fit parameters for ion–ion and ion–organic main group interactions are all incorporated in the MR part and set to zero in the SR (UNIFAC) part.

ACPD
8, 6069–6151, 2008

CC BY

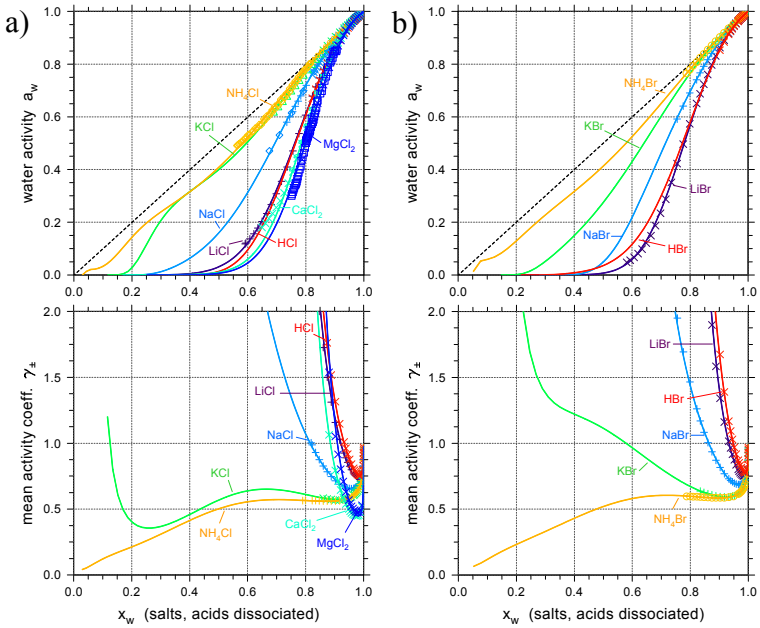

Fig. 3. Experimental (symbols) and modelled (solid lines) water activities and mean activity coefficients of the ions in binary aqueous salt (or acid) solutions at 298 K. The x-axis scale is the mole fraction of H_2O in the solution with respect to completely dissociated salts and acids. **(a)** Cl^-–electrolytes, **(b)** Br^-–electrolytes; data from: Robinson and Stokes (2002) (×), Hamer and Wu (1972) (+), Ha et al. (2000) (◊), Tang (1997) (△), Ha and Chan (1999) (□), Guendouzi et al. (2001) (⌓), and Covington and Irish (1972) (○). The diagonal, dashed line in the upper panels shows the water activity of an ideal mixture. At very high concentrations, beyond the efflorescence of supersaturated solutions, the curves are model predictions without direct experimental support.

ACPD
8, 6069–6151, 2008

CC BY

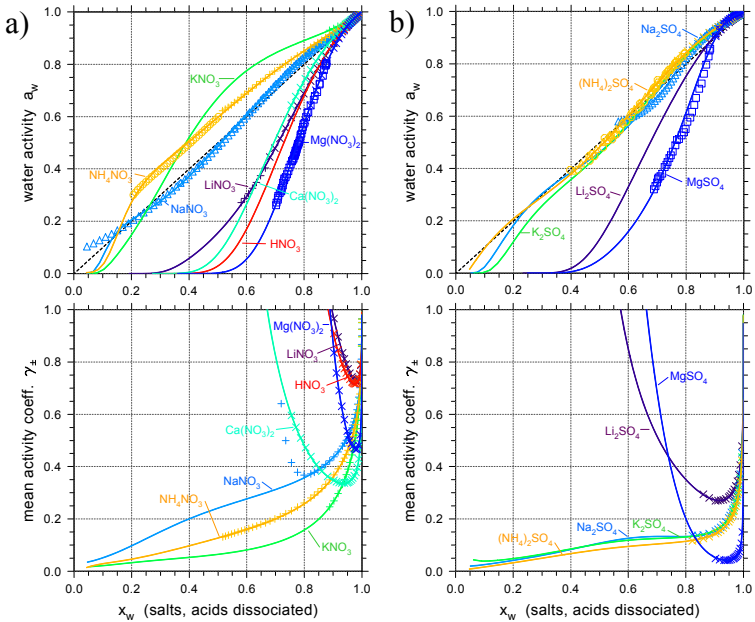

Fig. 4. Experimental (symbols) and modelled (solid lines) water activities and mean activity coefficients of the ions in binary aqueous salt (or acid) solutions at 298 K. **(a)** NO_3^-–electrolytes, **(b)** SO_4^{2-}–electrolytes; data from: Robinson and Stokes (2002) (×), Hamer and Wu (1972) (+), Ha et al. (2000) (◊), Tang and Munkelwitz (1994) (△), Ha and Chan (1999) (□), Guendouzi et al. (2003) (⌓), Chan et al. (1992) (○), and Clegg et al. (1995) (⬭). The diagonal, dashed line in the upper panels shows the water activity of an ideal mixture.

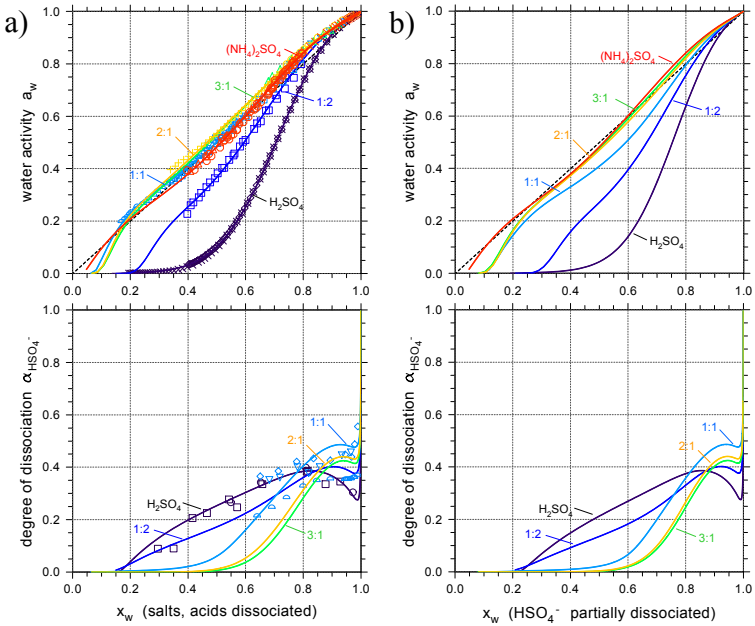

Fig. 5. Experimental (symbols) and modelled (solid lines) water activities of aqueous sulphuric acid, ammonium sulphate, and mixtures of both, indicated by the molar ratio of $(NH_4)_2SO_4$: H_2SO_4. The corresponding degrees of bisulphate dissociation, $\alpha_{HSO_4^-}$, are plotted in the lower panels. In **(b)** x_w on the x-axis is taking the modelled partial dissociation of bisulphate into account, while in (a) complete dissociation is assumed. **(a)** upper panel data from: Robinson and Stokes (2002) (×), Staples (1981) (◊), Kim et al. (1994) (□), Tang and Munkelwitz (1977) (▽), Clegg et al. (1995) (⬭), Spann (1984) (⌓), Tang and Munkelwitz (1994) (△), this study (bulk) (○), this study (EDB) (+). Lower panel data from: Knopf et al. (2003) (○), Myhre et al. (2003) (□), Young et al. (1959) (◊), Dawson et al. (1986) (▽), Irish and Chen (1970) (⌓).

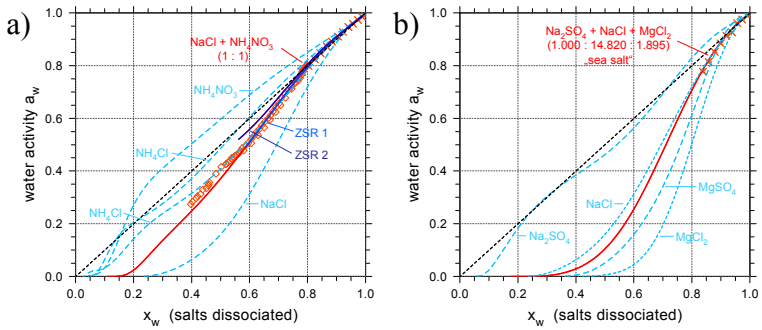

Fig. 6. Predictions and measurements of multi-salt mixtures. **(a)** salt mixture containing the four ions Na^+, NH_4^+, Cl^-, and NO_3^-. Symbols: (◊) EDB measurements (Ha et al., 2000), (×) bulk a_w measurements (this study). The red line is the AIOMFAC a_w prediction, the dashed lines show the model curves of the related binary salts. ZSR predictions are plotted for comparison using the polynomials given in Ha et al. (2000), assuming that the mixture is a solution of NaCl + NH_4NO_3 (ZSR 1) and $NaNO_3$ + NH_4Cl (ZSR 2), respectively. **(b)** "sea salt"-like mixture of Na^+, Mg^{2+}, SO_4^{2-}, and Cl^-. Experimental a_w data (×) from this study, AIOMFAC prediction (red solid line) and the AIOMFAC binary salts (dashed lines) for comparison.

ACPD
8, 6069–6151, 2008

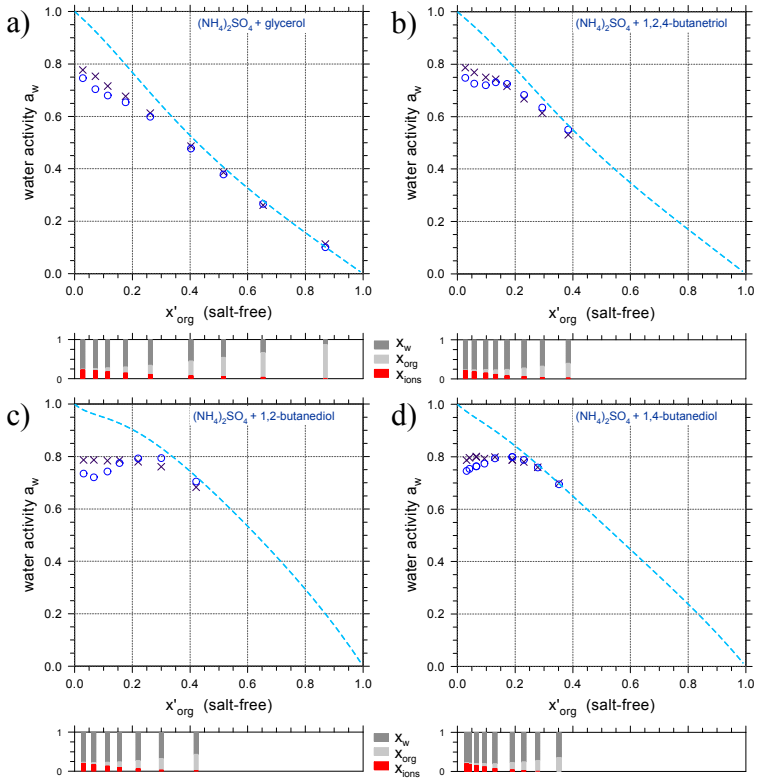

Fig. 7. Water activities of ternary polyol–water–ammonium sulphate mixtures at 298 K. (×) are experimental a_w data, (◯) AIOMFAC results. The dashed line is the AIOMFAC a_w of the salt-free solvent mixture. The ternary mixture compositions with respect to completely dissociated $(NH_4)_2SO_4$, are shown in the bar graphs (ions summed up). Polyols: **(a)** glycerol, **(b)** 1,2,4-butanetriol, **(c)** 1,2-butanediol, **(d)** 1,4-butanediol. Data from: Marcolli and Krieger (2006) (a) and (d), (this study) (b) and (c).

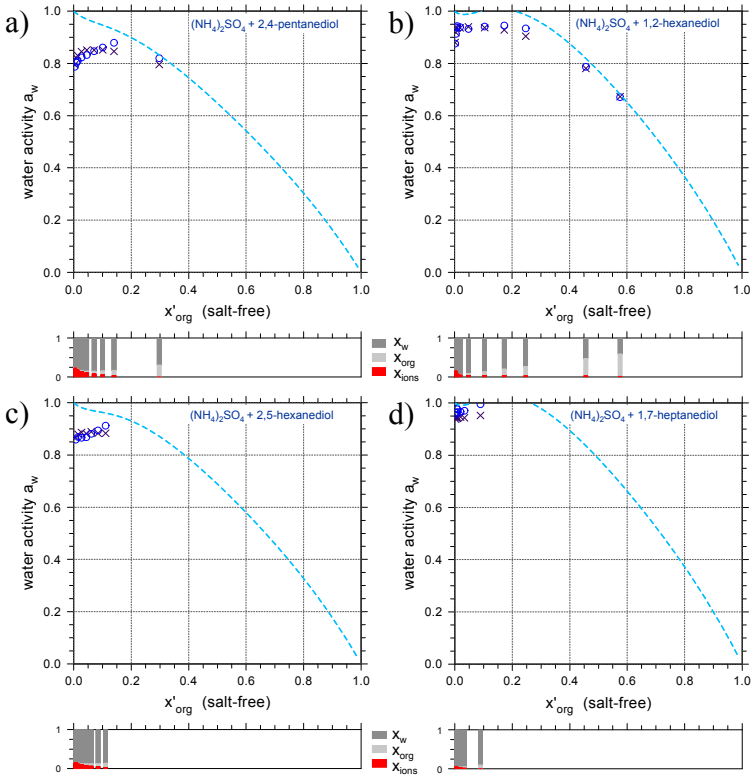

Fig. 8. Water activities of ternary polyol–water–ammonium sulphate mixtures at 298 K. (×) are experimental a_w data, (◯) AIOMFAC results. The dashed line is the AIOMFAC a_w of the salt-free solvent mixture. Polyols: **(a)** 2,4-pentanediol, **(b)** 1,2-hexanediol, **(c)** 2,5-hexanediol, **(d)** 1,7-heptanediol. Data from: Marcolli and Krieger (2006) (b), (this study) (a), (c), and (d).

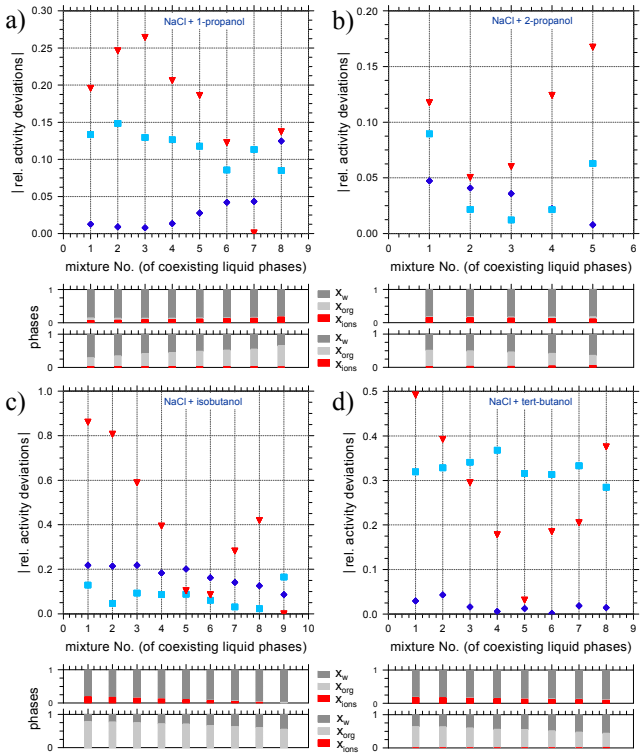

Fig. 9. Plots of the relative activity deviations between the two phases. LLE of alcohol–water–NaCl mixtures at 298 K. Plotted are the modelled relative deviations between the activities of the components in the two coexisting liquid phases. Symbols (□) alcohol, (◊) water, and (▽) mean ionic activities. The alcohols are: **(a)** 1-propanol, **(b)** 2-propanol, **(c)** isobutanol, **(d)** tert-butanol. The bar graphs show the corresponding phase compositions measured by: Chou et al. (1998) (a), Gomis et al. (1994) (b), Gomis et al. (1996) (c) and (d).

ACPD
8, 6069–6151, 2008

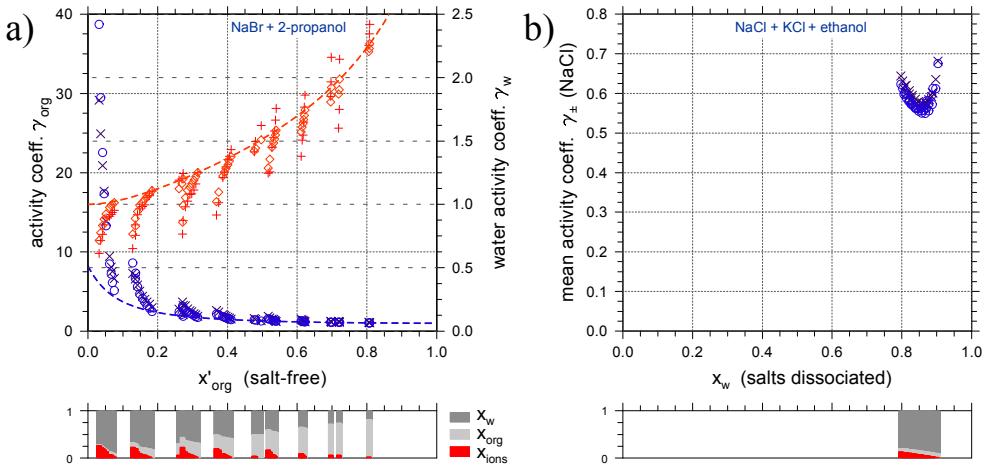

Fig. 10. **(a)** isobaric VLE of 2-propanol–water–NaBr mixtures at 353–358 K. Blue symbols: the measured (×) and calculated (◯) activity coefficients of 2-propanol. In red: measured (+) and calculated (◊) water activity coefficients. The dashed curves are the model results of the salt-free solvent mixtures. **(b)** Mean molal activity coefficients of NaCl in quaternary ethanol–water–NaCl–KCl mixtures from EMF measurements at 298 K. Symbols (◯) and (×) are AIOMFAC predictions and experimental data respectively. Data from: Morrison et al. (1990) (a), Farelo et al. (2002) (b).

ACPD
8, 6069–6151, 2008

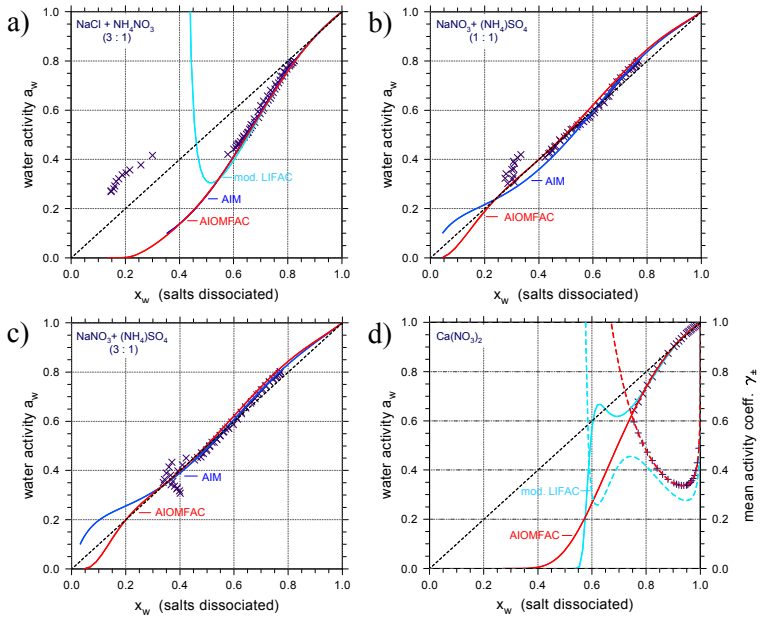

Fig. 11. Measurements of aqueous electrolyte solutions (symbols ×, +) and corresponding calculations of the models AIM III (Clegg et al., 1998b), mod. LIFAC (Kiepe et al., 2006), and AIOMFAC at 298 K. Salts: **(a)** NaCl + NH_4NO_3 at a molar salt mixing ratio of (3:1), **(b)** and **(c)** $NaNO_3$ + $(NH_4)_2SO_4$ (1:1) and (3:1), respectively, and **(d)** $Ca(NO_3)_2$. Since $(NH_4)_2SO_4$ is not parametrised in mod. LIFAC, (b) and (c) show only AIM and AIOMFAC water activities. $Ca(NO_3)_2$ is not available in the AIM, therefore (d) shows mod. LIFAC and AIOMFAC water activities (solid curves) and mean molal activity coefficients (dashed curves). Data from: Ha et al. (2000) (a), (b), and (c), Robinson and Stokes (2002) (d).

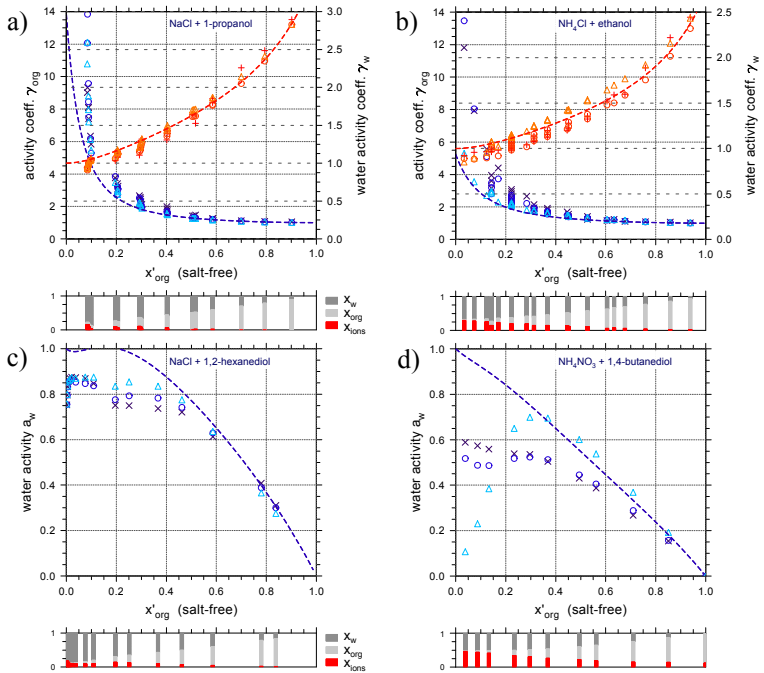

Fig. 12. Comparison of mod. LIFAC with AIOMFAC calculations for ternary alcohol/polyol–water–salt mixtures. Upper panels show alcohol and water activity coefficients from isobaric VLE data of **(a)** 1-propanol–water–NaCl mixtures at 360–365 K and **(b)** ethanol–water–NH_4Cl mixtures at 350–366 K. Symbols: measurements (×, +) and calculations of mod. LIFAC (△) and AIOMFAC (◯); in blue for the activity coefficients of the alcohols, in red for the activity coefficients of water. The dashed curves are the AIOMFAC results of the salt-free solvent mixtures. Panels **(c)** and **(d)** show measured and calculated water activities of 1,2-hexanediol–water–NaCl and 1,4-butanediol–water–NH_4NO_3 mixtures, respectively, at 298 K. Symbols as in the upper panels. Data from: Lin et al. (1993) (a), Johnson and Furter (1965) (b), Marcolli and Krieger (2006) (c) and (d).

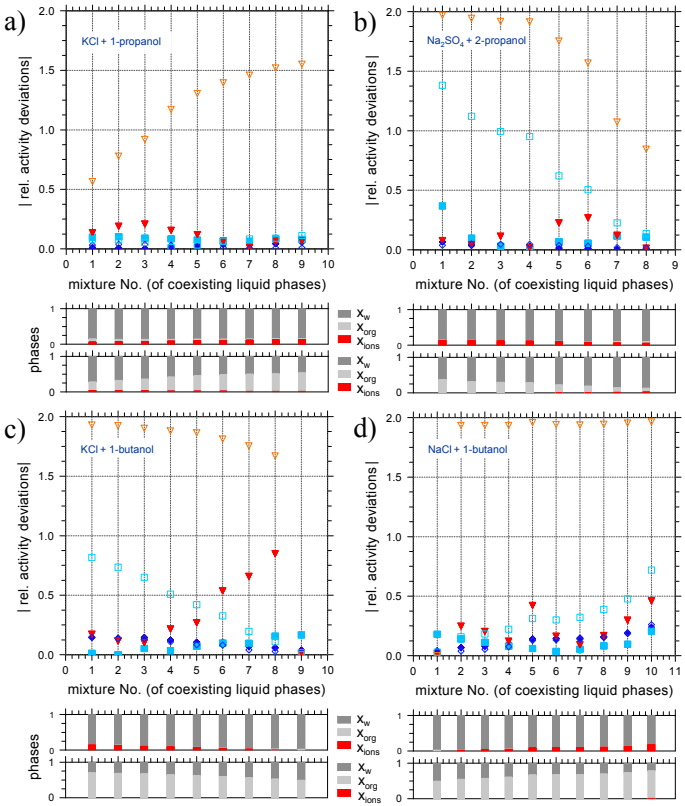

Fig. 13. Comparison of mod. LIFAC and AIOMFAC calculations for different LLE of alcohol–water–salt mixtures at 298 K. Plotted are the modelled relative deviations between the activities of the components in the two coexisting liquid phases. Symbols (□) alcohol, (◊) water, and (▽) mean ionic activities. Solid symbols show AIOMFAC, open symbols mod. LIFAC results. Mixtures: **(a)** 1-propanol–water–KCl, **(b)** 2-propanol–water–Na_2SO_4, **(c)** 1-butanol–water–KCl, **(d)** 1-butanol–water–NaCl. The bar graphs show the corresponding phase compositions measured by: Chou et al. (1998) (a), Lynn et al. (1996) (b), Gomis et al. (1996) (c), and Li et al. (1995) (d).